This is the peer-reviewed, final accepted version for American Mineralogist, published by the Mineralogical Society of America.
The published version is subject to change. Cite as Authors (Year) Title. American Mineralogist, in press.
DOI: https://doi.org/10.2138/am-2022-8213. http://www.minsocam.org/

Word count: 10915

Revision 1

Resolving the conundrum of equilibrium solubility of smectites

Stephen U. Aja†
Department of Earth and Environmental Sciences, Brooklyn College &
The Graduate Center, City University of New York,
2900 Bedford Avenue, Brooklyn, NY 11210-2889, U.S.A.
†, email: suaja@brooklyn.cuny.edu

This is the peer-reviewed, final accepted version for American Mineralogist, published by the Mineralogical Society of America.
The published version is subject to change. Cite as Authors (Year) Title. American Mineralogist, in press.
DOI: https://doi.org/10.2138/am-2022-8213. http://www.minsocam.org/

ABSTRACT

Smectites are common clay minerals in surface and near surface terrestrial environments and have recently been shown to be ubiquitous on Mars. Because these minerals are products of water-rock interaction, the thermodynamics of their interaction with fluids constitutes a vital part of resolving the utility of smectite mineralizations as petrogenetic and paleoenvironmental indicators on both Mars and Earth's near surface environments. Smectites, and other clay minerals of comparable compositional complexity, have been purported to be disequilibrium solids whose complexity derive from steep chemical gradients in their environments of formation rather than from crystal-chemical constraints. Solubility investigates of several natural smectites wherein none exhibited the predicted inverse correlation between pH – 1/3pAl and $pSi(OH)_4$ were adduced by May et al. (1986) as empirical proof of the disequilibrium solid concept and hence they asserted unequivocally that "it is obviously impossible to obtain valid ion activity quotients for smectite solubilities in these systems". However, the unattainability of equilibrium smectite solubility in those experimental systems was probably an artifact of the extremely high fluid-solid ratios employed therein. In subsequent experimental studies using significantly lower fluid-solid ratios, smectite-fluid interactions (Kittrick and Peryea, 1989; Gaboreau et al. 2020) and chlorite-fluid interactions (Aja and Dyar, 2002) yielded solubility data amenable to laws of chemical thermodynamics and thus invalidate the disequilibrium solid model. Therefore, the notion of smectite metastability and/or instability anchored on the disequilibrium solid model is false and warrants a more constrained definition of smectite metastability.

Keywords: smectite, metastability, disequilibrium solid, fluid-solid ratio, reversibility, solubility equilibrium, colloidal electrolyte

INTRODUCTION

Recent discoveries of the ubiquity of smectites on Mars (e.g., Chevrier et al., 2007; Ehlmann and Edwards, 2014; Bishop, 2018) and its potential for paleoenvironmental reconstruction of martian history underscores the need for an improved understanding of the thermodynamics of smectite-water interactions. In terrestrial environments, the smectite group of minerals are also common in soil environments and the Critical Zone, in argillaceous rock formations, as major component of bentonite deposits, in marine sedimentary environments, and in some hydrothermally-altered rocks (Borchardt, 1989; Chamley, 1989; Christidis and Huff, 2009; Wilson, 2013).

Smectites are 2:1-layer silicate minerals having an expandable structure and a certain amount of excess negative layer charge. They are divisible into dioctahedral and trioctahedral smectites; in the former, Al is the predominant octahedral cations though divalent ions may substitute for Al, and the various species include montmorillonites, beidellite and nontronite (Brown et al., 1978). In montmorillonites, layer charge stems primarily from substitutions in the octahedral sheet whereas for beidellite and nontronite (an iron analog of beidellite), tetrahedral charges predominate. Trioctahedral smectites include stevensite, hectorite, saponite and other less common species (such

as sauconite, volkhonskoite, swinefordite). The general structural formula for the montmorillonite – beidellite series is of the form $\left(Al_{2-y}Mg_y^{2+}\right)(Si_{4-x}Al_x)O_{10}(OH)_2M_{x+y}^{+} \bullet nH_2O$ where M^+, x and y represent the interlayer cation, tetrahedral substitution, and octahedral substitution, respectively. End-member smectite compositions are rare in nature but are defined, per half unit cell, as follows:

Beidellite	$M_x^+(Al_2)(Si_{4-x}Al_x)O_{10}(OH)_2$
Nontronite	$M_x^+(Fe_2^{3+})(Si_{4-x}Al_x)O_{10}(OH)_2$
Montmorillonite	$M_x^+(Al_{4-x}Mg_x)(Si_4)O_{10}(OH)_2$

Values of x reportedly lies between 0.65 and 1.3 per full unit cell (Brown et al., 1978). The extensive compositional variations typical of aluminous dioctahedral smectites lead to the definition of compositional fields (Figure 10 in Güven, 1988) for the following smectites: 1) Wyoming-type montmorillonite, 2) Otay-type montmorillonite, 3) Chambers-type (aka Cheto-type) montmorillonite, 4) Tatatilla-type montmorillonite, 5) "Non-ideal" (Fe-rich) montmorillonite, 6) Beidellite, 7) "Non-ideal" (Fe-rich) beidellite. The Cheto- and Wyoming-montmorillonite seem to be the predominant species amongst natural dioctahedral aluminous smectites (Güven, 1988). The actual compositional variation in natural smectite or illite may, however, be more limited than implied by reported analyses inasmuch as the structural formulae of clay minerals have generally been derived from bulk compositions of clay mineral powders rather than from chemical analyses of single crystals (Ransom and Helgeson, 1993).

Owing to questions of fundamental scientific curiosity and smectite applications in various industries, the thermodynamics of smectite-fluid interaction has been of continuing research interests; recent investigations have measured smectite dissolution kinetics (Cama et al. 2000; Köhler et al., 2005; Metz et al. 2005; Gainey et al. 2014; Cappelli et al. 2018; Di Pietro et al. 2020) and equilibrium solubility (May et al., 1986; Kittrick and Peryea, 1988, 1989; Peryea and Kittrick, 1986; Gaboreau et al. 2020). Phase equilibrium studies driven by performance assessment of bentonite in high-level nuclear waste (HLW) repositories have also been undertaken (Savage et al. 2019; Baron et al. 2019; Mosser-Ruck et al. 2016). The proposed designs for some HLW disposal barrier systems (e.g., the Japanese and Swiss concepts) include steel containers and gives rise to the question of the effect of iron on montmorillonite stability and possible consequences on the long-term behaviors of the barrier system of the alteration of montmorillonite to either non-swelling layer silicates or to Fe-rich smectites; the paragenetic sequence in HLW repositories resulting from fluid-mineral equilibria of Fe-rich clay minerals systems has also been of interest (Wilson et al., 2006a, b).

Solubility techniques provide the primary means to directly determine probable chemical conditions of smectite formation considering that smectites and other clay minerals are products of water-rock interactions. However, long-standing questions persist on the certainty of equilibrium solubility of these clay minerals, probability of dissolution of clay minerals to points of thermodynamic equilibrium or even attainment of stead state

during dissolution rate studies. However, recently available experimental data suggest that properly designed solubility experiments can yield meaningful insight into the thermodynamic stability of clay minerals. In this contribution, therefore, fundamental questions pertaining to the equilibrium solubility of smectites and analogous complex minerals will be re-examined in light of recent solubility studies.

DISEQUILIBRIUM SOLID MODEL OF CLAY MINERALS

The disequilibrium solid/metastable model of smectites and other compositionally-complex clay minerals, initially postulated by Lippmann (1977; 1982), was rooted in the extensive compositional variations found in natural illites and montmorillonites; according to Lippmann (1982), this variability is unexpected for low temperature minerals inasmuch as a smaller range of solid solutions is typical of higher temperature systems. In the paragonite-muscovite and pyrophyllite-muscovite systems, a range of stable solid solutions, comparable to those found in clay minerals, are expected above the relevant solvus temperatures (600° and 800°C, respectively); below the solvus temperatures, mutual solubility of the end members is negligible unless the system is characterized by a solvus having a lower critical point which condition requires that the heat of mixing be exothermic. Previously, Lippmann (1977) had speculated that the existence of fractional subscripts in the structural formulae of illites and montmorillonites preclude the application of solubility product conventions to model the solubility behavior of such minerals; in this model, valid solubility products may only be

142 derived for phases with fixed chemical compositions and nonfractional subscripts and,
143 the solubility of such compositionally complex solid solutions must be defined in terms
144 of the partial solubility products of end-member components. Considering the large
145 number of the endmember minerals needed to define the solubility products, Lippmann
146 (1977, 1982) reasoned that these clay minerals must be disequilibrium solids that form
147 by precipitation from extremely supersaturated solutions. In other words, the wide
148 range of compositional variations characteristic of clay minerals do not derive from
149 crystal chemical constraints modulated by the intensive variables of their environments
150 of formation. Furthermore, Lippmann (1982) pontificated that the formation of illites
151 and montmorillonites under low temperature conditions must imply their metastability
152 on the presumption that the magnitudes of electrostatic excess lattice energies
153 calculated for the paragonite-muscovite and muscovite-pyrophyllite systems suggest a
154 significant solid miscibility gap at low temperatures.
155
156 In a purported validation of the disequilibrium/metastable solid model of clay minerals,
157 May et al. (1986) reported irrational solubility behavior in their dissolution investigations
158 of five natural smectites. They attempted to determine the aqueous solubilities of the
159 smectites between pH 5 and 8; the smectites included two samples from commercial
160 bentonite deposits and three samples from an A horizon from Hawaiian Vertisols. Their
161 samples were pretreated by washing portions of each sample with pH 5 buffered 4 M
162 sodium acetate solutions, hot hydrogen peroxide solution and then size-fractionation to
163 prepare smectite (< 0.2 μm size fraction) stock suspensions. Subsequent to prewashing

of the 1% smectite stock clay suspensions with 0.01 M $MgNO_3$ solution, the samples were then equilibrated with the 0.01 M $MgNO_3$ solution. Furthermore, these experiments were designed to demonstrate reversibility of solubility; the pH, $SiO_{2(aq)}$ and dissolved Al concentration in the equilibrating mineral suspensions were adjusted by the additions of nitric acid, silicic acid and aluminum nitrate stock solutions. The studies were conducted at 25 °C and $\mathrm{p_{O_2}} = 1\ \mathrm{atm}$. Chemographic evaluation of the solubility data, in pH - l/3pAl^{3+} vs. pSiO_2aq space, showed no correlation between these parameters (Figures 3 and 4 in May et al., 1986) which contradicts the predicted inverse correlation. In the experiments with bentonite samples, gibbsite appeared to control Al level whereas amorphous aluminum hydroxides appeared to precipitate in the Hawaiian soil samples.

In order to explain this irrational smectite solubility pattern, the data was modeled using the idealized system $\mathrm{H_2O} - (\mathrm{AlFe})\mathrm{Si_4O_{10}(OH)_2} - (\mathrm{AlM}_{3/2})\mathrm{Si_4O_{10}(OH)_2}$ by May et al. (1986). In this system, kinetic restrictions and incongruent dissolution of the smectites were presumed to preclude equilibrium solubility of complex aluminosilicates of variable composition along a solution saturation curve. Moreover, the irreversible solubility displayed by the smectites was speculated to be somewhat analogous to stoichiometric saturation postulated previously by Thorstensen and Plummer (1977). But stoichiometric saturation does not imply solubility behavior divorced from applicable chemical model. Rather, stoichiometric saturation implies that, in both laboratory experiments or natural settings, kinetic restrictions may cause minerals that exhibit

compositional variation in space and time to equilibrate with a fixed composition during a short-term geologic process. That is, compositional complexity cannot preclude the dissolution of a solid solution to a point of thermodynamic equilibrium in laboratory experiments but will rather constrain such phases to behave as discrete phases of fixed compositions. Nonetheless, the failure to demonstrate smectite equilibrium solubility in the study was presumed to provide an experimental validation of the disequilibrium solid model. This view of smectite metastability thus posits that the complex and fractional atomic site stoichiometries of smectites prevent strict adherence to the fixed ion activity product/equilibrium solubility principles (Lippmann 1977, 1982). Therefore, smectites and similar clay minerals (illites, chlorites, etc.) are not true thermodynamic phases whose solubility behavior are subject to thermodynamic models using mass action constraints but are heterogeneous, disequilibrium solids that persists in geochemical systems owing to kinetic restrictions.

The study by May et al. (1986) gave considerable impetus to much of the currently prevailing view that clay minerals are disequilibrium solids and/or metastable phases, or even unstable phases. For instance, Essene and Peacor (1995) reasoned (on the basis of those conclusions) that without an independent quantification of the effects of variable grain size, structure and composition, clay mineral solubility experiments cannot be relied upon in assessing equilibrium conditions and that clay minerals being comprised of sub-micrometer crystallites with complex physical and chemical characters cannot be shown to have attained equilibrium. They further expressed considerable

skepticism on the significance of clay minerals solubility investigations on the presumption of an elevated reactivity of fine particulates relative to macroscopic phases of equivalent compositions. Therefore, a corollary of the disequilibrium solid model is that solubility investigations of complex clay minerals cannot intrinsically yield valid thermodynamic properties (such as log K) and hence the considerable skepticisms regarding clay minerals solubility studies (cf. Blanc et al., 2013).

SOLUBILITY OF COMPOSITIONALLY COMPLEX CLAY MINERALS

Mineral solubility in aqueous fluids consists of heterogeneous multicomponent processes involving hydrolytic detachment of cations from solid phases, electrostriction changes in the coexisting aqueous electrolyte consequent on the transfer of the released ions into the aqueous phase, hydrolysis of high ionic potential ions, changes in aqueous ion speciation resulting from changing pH during equilibration and possible system-wide changes in redox potential; at equilibrium, however, the overall solubility reaction is subject to the Gibbs Duhem law ($VdP - SdT - \sum_i n_i d\mu_i = 0$). Under isothermal, isobaric conditions, the multicomponent equilibria become fixed by the chemical potential (μ_i) and number of moles (n_i) of the various reacting species. For any reaction, equilibrium constant (including the solubility product of a dissolution reaction) and the slopes of phase boundaries on chemical potential diagrams (such as ion activity diagrams) are derivable from the Gibbs Duhem relation (see Nordstrom and Munoz, 1994). Hence, if the disequilibrium solid model of smectites and other complex clay minerals espoused

by Lippmann (1977, 1982), May et al. (1986) and Essene and Peacor (1995) is valid, the Gibbs-Duhem relation cannot predict accurate models of ion activity quotients in aqueous solutions equilibrated with such solids. In particular, chemographic evaluation of clay minerals solubility data will be at variance with predictions based on the Gibbs-Duhem law. Clearly, equilibrium chemical thermodynamic models of mineral – fluid interaction, rooted in the Gibbs-Duhem relation, provides a rigorous test of the validity of the disequilibrium solid model of smectites and other clay minerals.

Chlorite – aqueous solution equilibria

The chlorite mineral group is structurally and chemically more complex than smectites (and illites) and thus provide an excellent test case to evaluate these fundamental questions on the validity of modeling clay-mineral solubility with equilibrium constant formalism. The stability of Fe-Mg chlorites has recently been investigated from a number of perspectives including their interaction with aqueous solutions (Aja, 2019a; Aja et al., 2015; Aja and Dyar, 2002; Aja, 2002; Aja and Small, 1999). In the hydrothermal experiments, chlorite-kaolinite mixtures were equilibrated with approximately equal weight of aqueous NaCl or $MgCl_2$ solutions. The experiments were designed so that the chlorite-kaolinite boundary will be approached from both undersaturation and oversaturation defined in terms of ion activity quotients. In none of the experiments were Al and/or Fe introduced into the starting aqueous solutions and in some experiments neither Mg nor Si was introduced into the starting solutions. In experiments in which Al, Fe, Si and Mg were not added to the starting solutions, these

metals could only have been released into the equilibrated solutions by the kaolinite-chlorite reaction. The results of the experiments show that the final solution compositions were in agreement regardless of the composition of the starting aqueous solutions (Figure 4 in Aja and Small, 1999).

Using the Windsor chamosite – kaolinite equilibrium as an example, models of the chlorite – kaolinite equilibria are given by equations 1 and 2 (table 1). Equation 1 is a complex, multi-component reaction that includes processes of compensating mineral dissolution, transfer of the released cations into aqueous solution, intrinsic system-wide adjustments of redox conditions, and aqueous ion speciation. At equilibrium, the chemical potential of each species is equal across the phases coexisting in the experimental system. Being a multicomponent system, at least a 7-dimensional space will be necessary to simultaneously depict the stability relationship under isothermal, isobaric conditions. In view of the obvious difficulty of such constructs, the serial projection onto pseudo-binary ion activity space presents a salutary alternative; internal consistency of the solubility data requires then that the measured and predicted slopes of the chemical potential diagrams must concur for each pseudo-binary section.

In $\log \frac{a_{Mg^{2+}}^{0.5}}{a_{H^+}}$ $vs.$ $\log a_{Al(OH)_4^-} \bullet a_{H^+}$ space (equation 2), the kaolinite – chlorite boundary is predicted to have a slope of -1.46. Best-fit analyses of the solubility data yielded a slope of -1.35(0.17) (r^2= 0.94) at 75 °C (figure 1a); at the 95% confidence level, there is no difference between the predicted and measured slopes. For the Mg chlorite-kaolinite

reaction, the predicted slope and the disposition of the experimental data in $\log \frac{a_{Mg^{2+}}^{0.5}}{a_{H^+}}$ $vs.$ $\log a_{Al(OH)_4^-} \bullet a_{H^+}$ activity space are in agreement (Figure 1b) but the shallowness of the slope precludes valid regression analysis. Considering the changing aqueous ion speciation with temperatures and all the major ions occurring in the experimental system, the chlorite – kaolinite boundary was also projected onto additional pseudo-binary ion activity spaces including $\log a_{Al(OH)_4^-} \bullet a_{H^+}$ vs $\log \frac{a_{Fe^{2+}}^{0.5}}{a_{H^+}}$ and $\log a_{Al(OH)_4^-} \bullet a_{H^+}$ vs $\log a_{Fe(OH)_{3\,(aq)}^{\circ}}$ (Figures 6 and 7 in Aja and Dyar, 2002); in the latter examples, the chemical equilibrium models and the solution equilibration data were demonstrably congruent. Thus, in chemical potential diagrams, the predicted and measured slopes of the chlorite-kaolinite boundaries were in agreement and verifies that the multicomponent criteria of fluid-solid equilibria imposed by the Gibbs-Duhem relation were satisfied.

The Windsor chamosite and low-Fe clinochlore are monomineralic natural chlorite samples whose detailed structural chemistries have been determined (Aja et al., 2015); these monomineralic phases proved to be the solubility-controlling phases despite the presence of fractional subscripts in their structural formulae and even vacancies in their structures. These structural and chemical complexities of the chlorite group of minerals did not preclude either rational solubility patterns or the demonstration of equilibrium solubility, which observations contradict the postulate of the disequilibrium solid model.

Rational solubility of smectites

Unlike the chlorite group of minerals, pure monomineralic samples of natural smectites are less readily available; common minor phases admixed with the smectites samples include a variety of silica phases together with other non-layer silicates. This constitutes a complicating factor in experimental studies inasmuch as some of these extraneous phases cannot be physically separated.

Kittrick and Peryea (1989) and Gaboreau et al. (2020) studied the solubility of two different smectites using contrasting experimental techniques. Kittrick and Peryea (1989) reacted aqueous 0.010 M $MgCl_2$ solutions previously equilibrated with gibbsite with 0.2 – 5 μm Mg-saturated Belle-Fourche montmorillonite (BF) with goethite and gibbsite; the experiments ran for 7 to 15 days. In the studies by Gaboreau et al. (2020), the solubilities of kaolinite KGa-2, smectite MX-80, Silver Hill illite (IMt-2), Santa Ollala vermiculite (SO) and chlorite CCa-2 were measured in aqueous 10^{-2} M NaCl (MX80, IMt-2, and KGa-2) and 10^{-2} M $CaCl_2$ (SO and CCa-2) solutions. The batch experiments lasted up to seven years, and used a liquid to solid (L/S) ratio of 24:1. Smectite MX-80, a Na-bentonite from Wyoming, contains only about 78% clay and additional minor phases (quartz, cristobalite, and amorphous silicas). The dissolution experiments (at 25°C and 40°C) were carried out in starting aqueous solutions having a pH of 5, and the attainment of equilibrium was presumed owing to the long duration of the experiments; the investigators also presumed that dissolution experiments

316 exceeding two years in duration will be at thermodynamic equilibrium based on the
317 flattening out of the dissolution rate.
318
319 The solubility data of BF, depicted in figure 2, was modeled using equation 3 (table 1).
320 Based on the solubility product convention (equation 4, table 1), a graphical evaluation
321 of the solubility data (in $2\mathrm{pH} - \mathrm{pMg}^{2+}$ vs. $\mathrm{pSi(OH)}_4^\circ$ space) should yield a straight line
322 with a positive slope of 6.99; a linear regression analysis of the solubility data returned
323 a value of 6.99 (1.09) (R^2 = 0.83) despite the short duration of the experiments. The
324 standard error probably reflects the scatter in the data and experiments of longer
325 duration may have minimized the scatter and better facilitate clustering of the data
326 around the best-fit line. Nonetheless, it is significant that the experimental data
327 validates the solubility model and that the inverse linear correlation between aqueous
328 silica concentration and ion activity ratio expected at equilibrium is evident in figure 2.
329
330 For smectite MX-80, equation 5 (Table 1) gives the solubility model adopted by
331 Gaboreau et al. (2020) whereas equation 6 (table 1) is an expression of the
332 corresponding mass action constraint. In figure 3a, the MX-80 solubility data have been
333 projected onto the $3\mathrm{pH} - \mathrm{pAl}^{3+}\mathrm{vs}\ \mathrm{pH_4SiO_4}$ space; the aqueous solute concentrations
334 tabulated by Gaboreau et al. (2020) were presumed to be approximately equal to the
335 ion activities considering the low ionic strength of the aqueous media (Ionic strength =
336 0.01 – 0.02 m) and the final low pH of the reacted solutions (4.9 to 5) and hence the
337 presumption that all aluminum is present as $Al^{3+}_{(aq)}$. Furthermore, in this analysis

thermodynamic properties such as equilibrium constants are not being extracted from the solubility data. The MX-80 solubility data conform to the equation (figure 3a):

$$3\mathrm{pH} - \mathrm{pAl}^{3+} = 1.88 \pm 0.50\ \mathrm{pH_4SiO_4} + 2.73 \qquad (7a)$$

At the 95% confidence level, the value of the best-fit slope, 1.88 (0.50), is consistent with the predicted slope, 2.01 (equation 6 in table 1). The low regression coefficient (R^2 = 0.78) and the relatively large standard error of estimate reflects both the scatter and sparsity of the experimental data. Nonetheless, the inverse linear correlation of silica and ion activity ratios (figure 3a) belies assertions of smectite predisposition to irrational solubility behavior. In their smectite solubility study, May et al. (1986) plotted their data on $\mathrm{pH} - \frac{1}{3}\mathrm{pAl}$ vs $\mathrm{pSi(OH)_4}$ ion activity diagram but none of the five smectites they investigated displayed the predicted inverse linear correlation (Figures 3 and 4 in May et al., 1986). Rather, values of $\mathrm{pH} - \frac{1}{3}\mathrm{pAl}$ were approximately constant and independent of aqueous silica concentrations; this suggested that smectite lacks a definable stability field. Contrariwise, equation 7a quantifies an inverse linear correlation of these solute parameters from smectite MX-80 interaction with aqueous solution and thus, the outcomes of the investigations of May et al. (1986) and Gabreau et al. (2020) seem diametrically opposed.

However, the MX-80 solubility data lacks internal consistency which is a critical shortcoming. When the MX-80 solubility data is projected onto the 2pH-pMg^{2+} vs. pH_4SiO_4 ion activity space (figure 3b), the equation of the best fit line (R^2 = 0.63) is,

This is the peer-reviewed, final accepted version for American Mineralogist, published by the Mineralogical Society of America.
The published version is subject to change. Cite as Authors (Year) Title. American Mineralogist, in press.
DOI: https://doi.org/10.2138/am-2022-8213. http://www.minsocam.org/

$$2\mathrm{pH} - \mathrm{pMg}^{2+} = 1.50 \pm 0.57\ \mathrm{pH_4SiO_4} - 0.07 \quad (7b)$$

Though an inverse linear correlation is also evident, the slope of the best fit line 1.50(0.57) is at odds with the predicted slope of 17.47. This discordance is inconsistent with demonstrated patterns in prior solution equilibration investigations of illites and chlorites. Typically, solution equilibria of multicomponent clay minerals are characterized by the collinearity of solution data (cf. Aja et al. 1991b) where collinearity derives from crystal chemical controls on mineral chemistry. Whilst the reason for this lack of internal consistency of the MX-80 data is not clear, it raises questions on the efficacy of the particular static batch techniques utilized; other germane questions pertaining to the determination of the thermodynamic stability of smectites include the possible effects of structural disorder (turbostratic stacking) and variable morphologies (Brindley, 1980; Güven, 1988) as well as the compositional complexity of smectites.

On balance, the experimental data and the theoretical solubility model of the Belle Fourche montmorillonite, rooted in the Gibbs-Duhem relation, are concurrent in spite of the short duration of the experiments (7-15 days). By contrast, the smectite MX-80 solution data suggests smectite – aqueous solution equilibrium but lacks internal consistency despite the long duration (1 – 2500 days) of the experiments. This possibly reflects the contrasting experimental techniques, viz solution equilibration and hydrolytic dissolution. In addition, these two experiments used significantly different fluid-solid ratios. In the current context, it is significant that both studies yielded

rational solubility patterns and suggests that equilibrium can be demonstrated for suitably designed smectite – water interaction experiments even at 25 °C.

Latent solubility-controlling phases

The interpretation of mineral solubility data presents more challenges if the solubility-controlling phases differ from the composition of the starting mineral. For example, in experimental investigation of (less than 2-µm size fraction) K-saturated SWY-1 montmorillonite, the measured and predicted solubility models were divergent (Kittrick and Peryea, 1989); in $\mathrm{pH} - \mathrm{pK}^{+}$ vs. $\mathrm{pSi(OH)_4^{\circ}}$ coordinates, their experimental data returned a slope of 3.3 rather than the theoretical slope of 5.8 based on the bulk composition of the sample. Such discordant results may either indicate lack of sample equilibrium during the solubility study or that the solubility-controlling phase is different from the presumed composition of the equilibrated clay mineral.

Discordance between the bulk composition of investigated clays and composition of the solubility-controlling phase is further exemplified by the solubility studies of SO vermiculite and chlorite CCa-2 (Gaboreau et al., 2020). For the Santa Ollala vermiculite (SO) and chlorite CCa-2, equations 8 and 10 (table 1) are respectively the postulated solubility models whereas the corresponding equilibrium constant expressions are given by equations 9 and 11 (table 1). The solubility data for Santa Ollala vermiculite at 25 °C (figure 4a) shows a high degree of linearity (R^2 = 0.97) and the best fit equation is:

$$2\mathrm{pH} - \mathrm{pMg}^{2+} = 9.63 \pm 0.82\ \mathrm{pH_4SiO_4} - 19.55 \qquad (12)$$

This is the peer-reviewed, final accepted version for American Mineralogist, published by the Mineralogical Society of America.
The published version is subject to change. Cite as Authors (Year) Title. American Mineralogist, in press.
DOI: https://doi.org/10.2138/am-2022-8213. http://www.minsocam.org/

The value of the empirical slope, 9.63(0.82), diverges significantly from the predicted value of 1.12 (equation 9). For chlorite CCa-2, the best fit equation of the solubility data (figure 4b) is,

$$2\mathrm{pH} - \mathrm{pMg}^{2+} = -3.37 \pm 0.84\ \mathrm{pH_4SiO_4} + 18.99 \qquad (13)$$

The negative slope of equation 13, -3.37(0.84), is starkly different from the predicted positive value of 0.89 (equation 11). As was the case with SO, the divergence between the predicted and measured slopes suggests that the postulated solubility models (adopted by Gaboreau et al., 2020) do not apply. That is, the presumption that solubility was controlled by phases having the same compositions as the bulk compositions of the starting minerals appears erroneous. Furthermore, figure 4c show that the ion activity ratios of the final solution compositions for SO and CCa-2 overlap suggesting chemical similarities in the identity of the solubility controlling phases.

It is curious that despite the similarity of the initial experimental conditions for the three complex layer silicates (MX-80, SO and CCa-2) studied by Gaboreau et al. (2020) and considered in this review, only smectite MX-80 solubility data conform somewhat to the theoretical model. During the 7-year reaction time with the immanent aqueous solution, MX-80 dissolution engendered minimal pH changes (from 5.3 to 5.0, Table 6 in Gaboreau et al., 2020) whereas the dissolution of CCa-2 and SO were accompanied by significant pH changes; the pH changed from 5.2 to 7.3 and from 5.3 to 6.2 for SO and CCa-2, respectively. Hence, Al^{3+} is not likely to be the dominant Al species in those reacted solutions (see May, 1978). Probably, the solubility pattern observed for CCa-2

and SO typify laboratory weathering trajectories for these minerals under moderately acidic conditions whereas MX-80 solubility behavior reflects a confluence of factors. MX-80 contains 5.53% amorphous silica plus 8.29% cristobalite and 8.29% quartz in addition to the montmorillonite clay (Table 2 in Gaboreau et al., 2020); by contrast, CCa-2 contains neither amorphous silica nor cristobalite whereas SO contains only 0.2% cristobalite and 0.3% quartz. Secondly, in terms of structural chemistry, MX-80 has 3.738 Si atoms per half unit cell whereas SO and CCa-2 have 2.778 $Si/O_{10}(OH)_2$ and 2.635 $Si/O_{10}(OH)_8$, respectively. Because montmorillonite is comparatively a silica-rich phase, it's stability would be favored in aqueous silica-enriched environments. Conceivably, the contemporaneous dissolution of the extraneous silica phases contained in MX-80 sample, particularly the amorphous silica, would lead to elevated aqueous silica levels in the immanent solution. That is, the aqueous silica pumped in by the dissolution of amorphous silica would have fostered a stabilizing milieu for equilibration of the starting MX-80 montmorillonite. Such a scenario is consistent with the demonstrated expansion of the field of smectite stability, at the expense of other phases, when the concentration of aqueous silica in coexisting aqueous solution increases towards amorphous silica saturation limit (Aja et al., 1991a). By contrast, this extraneous buffering of silica levels in the bathing aqueous solution would be nonexistent for SO and CCa-2. Hence, the comparatively different solubility behaviors of MX-80, SO and CCa-2 in identical initial pH conditions reflect the possible range of outcomes in solubility studies of complex clay minerals. Serendipitously, however, the outcome of the interaction of smectite MX-80 with hydrothermal solutions affirm that

446 smectites do indeed have stability fields which are accessible by solubility
447 measurements.
448
449 # DISCUSSION
450 From the foregoing, layer silicates may exhibit three types of solubility characteristics
451 during laboratory investigations: 1) rational solubility for which the stoichiometry of the
452 reacted clay models the solubility characteristics, 2) rational solubility patterns wherein
453 the bulk composition of the equilibrated clay is at variance with the solubility data, and
454 3) irrational solubility pattern. The second group of behaviors result when either new
455 solubility-controlling phases formed during the course of the experiments or the sample
456 is a multiphase mixture and the solubility controlling phase has a different composition
457 relative to the bulk phase composition. The smectite solubility study reported by May et
458 al. (1986) is perhaps a well-known example of the third type of behavior; because their
459 study was a meticulous one, advancing a plausible explanation for their findings not
460 only has consequential heuristic purposes but also dispenses with the confusion bred by
461 the view of smectite-water interaction generated therefrom. The key to understanding
462 that irrational solubility behavior appears to be the fluid-solid ratio employed in those
463 investigations.
464
465 ## Fluid-solid ratio and clay minerals solubility
466 Table 2 provides a comparative overview of fluid – solid ratios used in some recent
467 solubility studies and it is evident that May et al. (1986) employed an extremely high

fluid-solid ratios, 100:1, in their study; this very high ratio contrasts markedly with the fluid-solid ratios utilized by all other investigators. They reacted 1% smectite (< 0.2 μm size fraction) suspension using 0.01 M $Mg(N0_3)_2$ solution as the background electrolyte. By contrast, fluid-solid ratios of approx. 1:1 and 24:1 were utilized in the study by Kittrick and Peryea (1989) and Gaboreau et al. (2020), respectively. That is, smectite investigations in which low fluid-solid ratios were used yielded rational solubility data consistent with chemical models whereas the experiments conducted with very high fluid-solid ratios generated irrational data. This suggests that the high fluid-solid ratios (used by May et al., 1986) may have hindered equilibrium by lengthening the duration of system-wide mineral-fluid interaction required to bring the volume of coexisting aqueous solution to equilibrium. If so, then the conditions of the experiments constituted kinetic barriers to attainment of equilibrium and the failure to attain equilibrium is an artifact of the experimental condition rather than an evidence of intrinsic metastability or instability of smectites.

The high-fluid ratios in those solubility experiments apparently generated finely-dispersed smectite suspensions. Typically, when dispersed in water, smectites undergo both hydration and osmotic swelling during which the basal spacing increases. With increased osmotic swelling, finely dispersed montmorillonite suspensions become colloidal electrolytes whose charge result from ionization (Foster, 1954; Norrish, 1954; Smalley, 1994). The exchangeable cations dissociate from the anionic 2:1 layer framework and tend to form a diffuse double layer whereas the negatively charged

framework units tend to repel each other. The osmotic swelling of the colloidal suspension is differentiated into the isotropic stage, an anisotropic stage and a transitional stage between the two (McBride and Baveye, 2002); the isotropic stage occurs at clay content of approximately 0.02% to 5% clay suspension whereas clay suspensions of the anisotropic stage have about 6% or more (i.e., $\gtrsim$ 6%) montmorillonite content. The dispersed clay platelets in the isotropic stage lack structural order. Certainly, this phenomenon is more clearly understood for Na montmorillonite whereas for smectites having divalent cations as exchangeable cations (such as was used by May et al., 1986), the osmotic swelling is limited relative to that of Na montmorillonite suspensions (Slade and Quirk, 1991). Nonetheless, the 1% clay suspension used by May et al. (1986) consigned the clay content of their experimental setting to the lower reaches of the isotropic stage; that is, the rather high fluid-solid ratios could have disposed their experimental clay suspension to an isotropic colloidal electrolytic state. Moreover, whether or not their chemical smectite purification protocols exacerbated the predisposition of the smectite samples towards colloidal electrolytic behavior is an unanswered question. It is conceivable, nonetheless, that the high fluid solid ratios utilized in that study imply that an isotropic colloidal electrolytic clay suspension does not exhibit mineral solubility characteristics expected of ordinary mineral-aqueous fluid mixtures.

Both May et al. (1986) and Kittrick and Peryea (1989) used Mg-saturated montmorillonite from bentonite deposits in their respective investigations but with very

different fluid-solid ratios (Table 2); the very low fluid-solid ratio in Kittrick and Peryea (1989) possibly minimizing formation of smectite colloidal electrolytes whereas the reverse would have been the case for the rather high ratio of May et al. (1986). In seeking to explain their observations, May et al. (1986) concluded that "it is obviously impossible to obtain valid ion activity quotients for smectite solubilities in these systems …". However, this assertion did not consider that their experimental systems may have been isotropic colloidal electrolytic suspensions, and their findings are averse to the inferences from other studies (Gaboreau et al., 2020; Peryea and Kittrick, 1989). In fact, the Mg-saturated BF conformed to the monophase model of smectites in which the interlayer cation and the 2:1 layer framework constitute a single structural unit. Hence, these latter studies directly contradict the assertion by May et al. (1986). Remarkably, these three investigations (Gaboreau et al., 2019; Kittrick and Peryea, 1989; May et al., 1986) included smectites from bentonite deposits. All of the natural smectite specimens contain minor mineral components or impurities and the inference that these trace components may have precluded access to equilibrium ion activity quotients in the equilibrated solutions (as espoused by May et al., 1986) is not borne out by these latter studies. The irrational smectite solubility data reported by May et al. (1986) appears rooted in the rather high fluid-solid ratio used in that study and may also reflect sluggishness of equilibration rate owing to the large fluid volume used in the study and the apparent colloidal electrolytic nature of the suspension.

This is the peer-reviewed, final accepted version for American Mineralogist, published by the Mineralogical Society of America.
The published version is subject to change. Cite as Authors (Year) Title. American Mineralogist, in press.
DOI: https://doi.org/10.2138/am-2022-8213. http://www.minsocam.org/

533 The Gibbs-Duhem relation, a fundamental law of chemical thermodynamics, describes
534 all and necessary conditions of mineral-water equilibrium regardless of whether the
535 equilibrium is stable or metastable. Under isothermal and isobaric conditions, the law
536 reduces to,

537 $$\sum_i n_i d\mu_i = 0 \qquad (14)$$

538 Hence, equilibrium constants of chemical reactions, solubility products of dissolution
539 reactions and slopes of phase boundaries in ion activity diagrams are derivable from
540 this law; the number of moles of each reacting species is same as the absolute values
541 of the stoichiometric coefficient of each species in a given chemical reaction (see
542 Nordstrom and Munoz, 1994). In other words, the Gibbs-Duhem law is violated if the
543 measured slope (of a phase boundary in ion activity diagram) disagrees with the
544 predicted slope for a particular chemical model or, alternatively, the model is either
545 wrong or does not apply. For example, the slopes predicted for the solubilities of Santa
546 Ollala vermiculite (Equation 9) and chlorite CCa-2 (Equation 11) vary significantly from
547 the slopes obtained from chemographic evaluation of the data. This suggests that a
548 different chemical model applies to the solubility data or that different solubility
549 controlling phases buffered solute concentrations; such outcomes underscore the need
550 for exhaustive characterization of the solid products from solubility investigations by
551 analytical transmission electron microscopy as a way to verify the identity of the
552 neoformed phases (cf. Yates and Rosenberg, 1998). As has been demonstrated, the
553 solubility data for Belle Fourche montmorillonite (figure 2), MX-80 smectite (figure 3a),
554 Windsor chamosite (figure 1a) and low-Fe clinochlore (figure 1b) conform to the

555 predictions of the Gibbs-Duhem law; these concurrences validate the respective models
556 of solubility equilibria. Furthermore, hydrothermal experiments conducted with various
557 illites and sericites similarly demonstrate mineral-fluid equilibria (see discussions in Aja,
558 2019b). That this array of clay minerals (smectites, illites, sericites and chlorites) obey
559 laws of chemical thermodynamics in their interaction with hydrothermal solutions is
560 diametrically opposed to the postulate that clay mineral solubility experiments cannot
561 be relied upon in assessing equilibrium conditions and cannot be shown to have
562 attained equilibrium. In addition, the proposition by Essene and Peacor (1995) that the
563 complex physical and chemical characteristics of sub-micrometer crystal sizes of clay
564 minerals preclude their behavior as genuine thermodynamic phases in solubility studies
565 is demonstrably false.
566
567 **Pitfalls in designing solubility studies**
568 Both hydrolytic dissolution and solution equilibration techniques provide unique tools to
569 assess the relative stabilities of clay minerals but a successful application of these
570 requires awareness of both the limitations and potential. An extremely valuable list of
571 experimental and conceptual deficiencies that could limit the utility of clay minerals
572 solubility studies were listed by May et al. (1986) whereas possible criteria to assess
573 equilibrium solubility studies were suggested by May and Nordstrom (1991). The
574 deficiencies include: 1) lack of proof of the attainment of equilibrium where equilibrium
575 has been inferred from extrapolation of solute activities to infinite time, 2) the use of
576 acidic equilibrating solutions in which minerals may be unstable, 3) the use of

inappropriate analytical techniques which neglect the role of ion speciation especially for Al^{3+}, 4) erroneous identification of solubility-controlling mineral species, and 5) uncertainties in the role of exchangeable cations in smectites; possible indicators for equilibrium in solubility studies include a) reaction reversibility of equilibrium solubility, b) validation of stoichiometric mineral solubility by the invariance of equilibrium constant over an appropriate range of solute activities, c) absence of consequential interference from secondary reactions, and d) a well characterized solid phase that does not undergo compositional alteration during the dissolution reaction. Clearly, these equilibrium criteria apply to monomineralic samples which may not always be available for clay minerals but notwithstanding, the need to affirmatively demonstrate attainment of equilibrium in solubility studies is of primary concern.

Reversibility of ion activity ratios in equilibrated solutions has been employed as an experimental strategy to demonstrate equilibrium solubility (Kittrick, 1982; Kittrick, 1984; May et al., 1986; Sass et al., 1987; Kittrick and Peryea, 1989; Aja and Small, 1999; Aja and Dyar, 2002). Recently, however, Blanc et al. (2013) and Gaboreau et al. (2020) postulated that, in clay minerals solubility investigations, equilibrium should be assessed using ion activity products (IAP) calculated via standard state Gibbs free energy of formation derived from calorimetric measurements of the particular clay minerals. The rationale for this approach is that calorimetry derived IAP's are independent of mineral-water interactions and thus circumvent questions of attainment of equilibrium inherent in solubility techniques. Certainly, the combined application of

599 solubility techniques and calorimetry to determine the thermodynamic properties of clay
600 minerals is not novel (Hemingway et al. 1984, Kittrick, 1982; Aja 2019a, Aja et al.,
601 2015) but certain limitations attend the approach adopted by Gaboreau et al. (2020) to
602 ascertain equilibrium solubility. In the first instance, the adoption of equilibrium
603 solubility verification parameter external to the system under investigation (such as by
604 calorimetry-based IAP) is a tacit determination that the Gibbs-Duhem relation does not
605 provide the empirical yardstick needed to assess equilibrium in clay minerals-fluids
606 experimental investigations. Effectively, this is a substantive adoption of an independent
607 quantification of equilibrium in clay mineral solubility studies propounded by Essene and
608 Peacor (1995) and hence, is a de facto subscription to the disequilibrium solid model.
609 Furthermore, calorimetry is taken for bulk sample materials and natural clay minerals
610 such as illites and smectites are rarely monomineralic and minor phases that constitute
611 less than 5% of the sample may be poorly represented in a modal mineralogy of the
612 sample based on XRD. That is, calorimetric measurements of natural clay mineral
613 samples require correction for modal mineralogy which may be subject to inaccuracies.
614
615 An inherent limitations of the approach adopted by Gaboreau et al. (2020) is
616 encapsulated in the seven to nine orders of magnitude deviation of calorimetry-derived
617 equilibrium constants from solubility-derived IAP (Figures 6 and 7 in Gaboreau et al.,
618 2020). For CCa-2, calorimetric data yielded a solubility product (log K) of 61.31(1.3) at
619 25 °C whereas log IAP derived from measured solute activities was 52.97(0.9); the
620 corresponding values for SO are 44.77(1.4) and 37.99(0.7), respectively (Table 9 in

Gaboreau et al., 2020). Even after a 7-year duration of the dissolution experiment at 25 °C, solubility-derived log IAP values for SO and CCa-2 still lie outside the theoretically-calculated log K±2σ envelope (Figure 9 in Gaboreau et al., 2020). Not only does this manifest the shortcomings of indirectly and externally quantified equilibrium, it simultaneously validates the prior deduction, based on chemographic analysis (figure 4, this study), that the solubility data for SO and CCa-2 contradict the presumed solubility models. Because the predicted slopes for the solubility models for SO and CCa-2 are significantly at odds with the experimental data, the compositions of the solubility-controlling phases are unknown. Therefore, comparing solubility-based IAP values and calorimetry-based solubility products, when the identity of the solubility-controlling phase is not known, is devoid of physical reality. This does not imply an intractable difficulty in solubility studies of these complex minerals considering that in studies with minerals of comparable complexity, equilibrium solubility has been demonstrated using reversibility of ion activity quotients. For instance, significant pH changes accompanied the equilibration of Mg-chlorite-kaolinite mixtures (Aja and Small, 1999) and Fe-chlorite – kaolinite mixtures (Aja and Dyar, 2002). Yet, reversibility of ion activity ratios (Figures 5 and 6) permitted location of the positions of the phase boundaries and, the predicted and measured slopes of the phase boundaries for the chlorite-kaolinite equilibria in different pseudo-binary sections were consonant with chemical equilibrium models. Evidently, stability studies designed to demonstrate solubility equilibrium via the chemistries of equilibrated aqueous solutions and to thus determine unambiguously the

chemistries of aqueous fluids in which the clay minerals are stable seem preferable as an experimental approach.

The application of secular variation of dissolution rate as an equilibrium metric also suffers from the inability to locate the position at which the Gibbs free energy of reaction is minimized. Consider for instance the solubility of kaolinite KGa-2 reported by Gaboreau et al. (2020). Though there seems to be a broad demonstration of the utility of solubility techniques in the determination of conditions of equilibrium solubility of kaolinite (Kittrick, 1966, 1969; May et al. 1986; Devidal et al, 1996), the KGa-2 solubility data seems to be somewhat at variance with this. (Given that the KGa-2 study was conducted in a 0.01 m ionic strength solution whose final pH values varied from 5.0 (day 1) to 4.2 (day 2500), it will again be assumed that the reported molal concentrations approximate ion activities). Figure 7 depicts the solubility data in 3pH – pAl^{3+} vs. pH_4SiO_4 space; at the 95% confidence level, the slope of the best fit line, 2.22(0.63), is greater than the predicted slope of 1.0 for stoichiometric kaolinite dissolution. A line having the appropriate slope could be emplaced amongst the data (Figure 7) though a multiplicity of such lines is applicable. Thus, the locus (in ion activity space) of minimal Gibbs free energy of the dissolution reaction ($\Delta G_r = 0$) cannot be determined unambiguously from their data; that is, the univariant boundary separating the divariant fields (solution field vs. kaolinite + solution field) is not uniquely defined by their solubility data.

Conceivably, equilibrium could be presumed for the 7-year KGa-2 solubility measurements; log IAP values obtained from the solubility data, 6.61(0.7), and the calorimetry-based kaolinite solubility product (log K), 6.46(0.6), are in agreement (see Table 9 in Gaboreau et al., 2020). However, the attainment of equilibrium solubility after 2500-days merely reflects this particular experimental setup. Contrariwise, equilibrium was demonstrated by reversibility of ion activity quotients after 1237 days in the solubility measurements of the Dry Branch kaolinite, (Figure 1 in May et al., 1986); in other words, equilibrium was attained in the Dry Branch kaolinite study in less than half the time required to attain equilibrium in the KGa-2 study. This contrast in the length of time required to attain equilibrium begs the question of the possible effect of fluid-solid ratios on reaction rates. Though the fluid-solid ratios were of the same order of magnitude but the slight difference in the ratios, 20:1 (Dry Branch kaolinite; May et al., 1986) vs. 24:1 (kaolinite KGa-2; Gaboreau et al., 2020), appear to have had a significant effect. Of course, differences in crystallinity may also have played a role but the fluid-solid ratio may have been more consequential in regulating duration of experiments needed to attain equilibrium. Therefore, the inference that equilibrium clay solubility is attained after two years (Gaboreau et al., 2020) has no universal application but applies only to the particular conditions of the reporting experimental study. Secular variation in dissolution rates probably reflects, inter alia, the fluid-solid ratio of that particular experimental set up and whether or not equilibrium is attained and how long it takes to demonstrate such does not resolve questions on the stability vs. metastability of these phases. In conjunction, however, with the apparent effect of fluid-solid ratios

686 demonstrated in solubility of complex layer silicates, perhaps, fluid-solid ratio
687 approaching 1:1 may be ideal in clay minerals solubility investigations.
688
689 The case for designing these solubility investigations such that enough reversed
690 experimental data points are generated is self-evident; this assures meaningful
691 statistical treatment of the data under isothermal conditions, and would permit data
692 interpretation using a valid cluster analysis approach if statistical treatment is not
693 feasible. The validity of reversibility of ion activity quotients as an experimental design
694 strategy, during clay minerals solubility investigations, has been demonstrated for
695 kaolinite (Dry Branch, May et al., 1986), smectite (BF montmorillonite, Figure 2) and Fe-
696 Mg chlorites (Figures 5 and 6). Apparently, reversibility of ion activity quotients coupled
697 with equilibration of mineral mixtures present a superior experimental strategy relative
698 to hydrolytic dissolution (in the investigation of the stability of complex clay minerals)
699 inasmuch as the mineral reaction path is constrained. Additional benefit of experimental
700 designs employing reversibility is the possible identification of anomalous data;
701 reversibility of ion activity quotients that model equilibrium phase boundaries also attest
702 to the validity of the Gibbs-Duhem relation in defining fluid-mineral equilibria, even of
703 complex clay minerals.
704

705 False notions of metastability of clay minerals

706 Owing to the fine crystal sizes of clay minerals, the Gibbs free energies of systems
707 containing such may not be minimized because of the higher surface free energy

content relative to an identical system containing macroscopic phases. Clay minerals may thus be described as metastable phases in this narrow sense. The energy content in the low pressure – temperature conditions of their formation does not seem to be high enough to produce macroscopic crystals of clay minerals and in this sense the metastability is constrained (cf. Anderson, 2005) by the environment of formation. This concept of metastability is rigorous; however, metastability has also been applied somewhat pejoratively and presumptively to clay minerals occurrences and behaviors.

Metastability of clay minerals has tended to be used to describe poorly understood or confounding phenomenon such as the irrational smectite solubility discussed above. Results of some hydrothermal synthesis experiments have also been attributed to metastability even when the physicochemical conditions of the synthesis experiments were atypical of natural environments in which clays form; such interpretations emphasize the need for a more systematic definition of physiochemical conditions of clay minerals genesis. The wide compositional variation of clay minerals has also been regarded as expressions of metastability. In addition, Ostwald step rule has widely been presumed to provide the framework for thinking about clay minerals evolution during burial diagenesis (e.g., Morse and Casey, 1988; Essene and Peacor, 1995) despite the absence of corroborating empirical validation. Clearly, the pervasive application of metastability to poorly understood clay minerals phenomena and/or paragenesis hinders the development of a framework for understanding clay minerals evolution in space and time. Much of these presumptive notions have been predicated on the false

730 expectation that equilibria in clay-bearing systems will be analogous to features of
731 mineral equilibria characteristic of metamorphic conditions. This presupposition
732 underlies the model of Lippmann (1982), and has become propagated widely in the
733 literature leading to minimization of the peculiar characteristics distinguishing the low
734 temperature clay minerals environments from metamorphic ones (cf. Jeans, 2009). For
735 instance, biological activities play significant roles during weathering (in the Critical
736 Zone), neoformation and clay minerals authigenesis; in marine sediments, the
737 distribution of redoximorphic fronts and environments influences the general
738 distribution of some 2:1 clay minerals (Jeans, 2009). Furthermore, some clay minerals
739 form in settings subject to hydrodynamic fluxes and gradients atypical of metamorphic
740 environments. In fact, at high enough temperatures in geothermal systems ($T \gtrsim 300$
741 °C), illite crystallites form idioblastic mica by coalescence of the crystallites; this growth
742 mechanism has not been documented in lower temperature conditions implying that the
743 lower temperature systems may lack enough driving force for the development of
744 macroscopic layer silicate crystals. Understanding clay minerals evolution in space and
745 time mandates clarification of the parameters of their thermodynamic stability vis-à-vis
746 the kinetic effects on such stability relationship for which the irreversible
747 thermodynamic framework probably provides the most appropriate framework (Aja,
748 2019b).
749
750
751

This is the peer-reviewed, final accepted version for American Mineralogist, published by the Mineralogical Society of America.
The published version is subject to change. Cite as Authors (Year) Title. American Mineralogist, in press.
DOI: https://doi.org/10.2138/am-2022-8213. http://www.minsocam.org/

IMPLICATIONS

The foundational tenet of the disequilibrium solid model of complex clay minerals is that their compositional variations reflect steep chemical gradients in their environments of formation and thus their fractional atomic site occupancies, which is the typical compositional characteristic inherent in their structures, are not governed by physicochemical laws. Secondly, the disequilibrium solid model predicts that clay mineral-water interactions are not amenable to solubility product conventions given that such minerals form by precipitation from extremely supersaturated solutions. In addition, the disequilibrium solid model expresses solid solution models of clay minerals in purely electrostatic terms in which purely ionic solids models of silicate minerals are believed to accurately describes excess lattice energy functions of such solid solutions. Given that silicate minerals are not pure ionic solids and these compositionally complex clay minerals have been shown to exhibit rational solubility behaviors for which the resulting ion activity quotients are governed by solubility product conventions rooted in the Gibbs-Duhem law, the disequilibrium solid model of complex clay minerals should be presumed to have been debunked. For nearly half a century, the disequilibrium solid model and its corollaries have beclouded understanding of the thermodynamics of clay minerals-fluid equilibria and hence the need for vigorous research in this field aimed at significantly improving a working knowledge of both the intensive and extensive physicochemical variables controlling the thermodynamic stability of these complex clay minerals.

774 Smectites and chlorites are the most common phyllosilicates detected so far on Mars,
775 the former being of greater incidence. For instance, at Mawrth Vallis, thick, complex
776 profiles of phyllosilicates have been inferred from CRISM hyperspectral visible/near-
777 infrared spectra. The description of the mineral horizons (Fe^{3+}/Mg-smectite, ferrous
778 clays, sulfates, overlain in turns by a thin ferrous iron bearing clay unit, a salty and/or
779 acidic alteration phases and sulfates) imply changing environmental conditions in which
780 the layer of poorly crystalline aluminosilicates overlying the Al-rich phyllosilicate layer
781 possibly marks the end of the warm and wet environment on early Mars (Bishop et al.
782 2020). Such complex mineralization sequences on Mars suggest dynamic, steep
783 hydrochemical gradients, for which smectite-fluid interaction cannot furnish any insights
784 into their formation conditions if smectites are disequilibrium solids. But because the
785 disequilibrium solid model is invalid, investigations of smectite - fluid equilibria using
786 various types of solubility techniques hold important keys to understanding conditions
787 of smectites formation on Mars and their utility as petrogenetic indicators thereon.
788
789 ACKNOWLEDGEMENT
790 Constructive and helpful review comments by Dr. Jim Wilson are acknowledged. This
791 work was not directly funded by any external funding agencies.
792
793
794 Conflict of Interest
795 The author declares that he has no conflict of interests.
796
797
798 **REFERENCES**
799 Aja, S.U. (2002) The stability of Fe-Mg chlorites in hydrothermal solutions: II.
800 Thermodynamic properties. Clays and Clay Minerals, 50, 591–600.

Aja, S. (2019a) Excess functions of chlorite solid solutions and neoformation of Fe-chlorite: Some implications of recent thermochemical measurements. American Mineralogist, 104, 232–243.

Aja, S.U. (2019b) On the thermodynamic stability of illite and I-S minerals. Clays and Clay Minerals 67, 518–536.

Aja, S.U., and Dyar, M.D. (2002) The stability of Fe-Mg chlorites in hydrothermal solutions I. Results of experimental investigations. Applied Geochemistry, 17, 1219 - 1239.

Aja S.U., and Rosenberg P.E. (1992) The thermodynamic status of compositionally-variable clay minerals: A discussion. Clays and Clay Minerals, 40, 292-299.

Aja, S.U., and Small, J.S. (1999) The solubility of a low-Fe clinochlore between 25 and 175 ºC and $P_v = P_{H_2O}$. European Journal of Mineralogy, 11, 829 – 842.

Aja, S.U., Omotoso, O., Bertoldi, C., Dachs, E., and Benisek, A. (2015) The structure and thermochemistry of three Fe-Mg chlorites. Clays and Clay Minerals, 63, 351 – 367.

Aja, S.U., Rosenberg, P. E. and Kittrick, J. A. (1991a): Illite equilibria in solutions: I. Phase relationships in the system K_2O-Al_2O_3-SiO_2-H_2O between 25 and 250°C. Geochimica et Cosmochimica Acta, 55, 1353–1364.

Aja, S.U., Rosenberg, P.E., and Kittrick, J.A. (1991b): Illite equilibria in solutions: II. Phase relationships in the system K_2O-Al_2O_3-MgO-SiO_2-H_2O. Geochimica et Cosmochimica Acta, 55, 1365-1374.

Anderson, G.M. (2005) Thermodynamics of natural systems. 2nd edition, 648 pp. Cambridge University Press, New York.

Baron, F., Petit, S., and Decarreau, A. (2019) Experimental evidence of the metastability of ferric smectite. Geochimica et Cosmochimica Acta, 265, 69–84.

Bishop, J.L., 2018. Chapter 3: remote detection of phyllosilicates on Mars and implications for climate and habitability. In: Cabrol, N.A., Grin, E.A. (Eds.), From Habitability to Life on Mars. Elsevier, pp. 37–75.

Bishop, J. L., Gross, C., Danielsen, J., Parente, M., Murchie, S. L., Horgan, B., Wray, J. T., Viviano, C., and Seelos, F. P. (2020) Multiple mineral horizons in layered outcrops at Mawrth Vallis, Mars, signify changing geochemical environments on early Mars. Icarus 341, 113634

Blanc, P., Vieillard, P., Gailhanou, H., and Gaboreau, S. (2013) Thermodynamics of Clay Minerals In F. Bergaya and G Lagaly, Eds., Handbook of Clay Science, 5, 173-210. Elsevier.

Borchardt, G. A. (1989) Smectites In J.B. Dixon and S.B. Weed. Eds., Minerals In Soil Environments, 2nd ed., 675‑727. Soil Science Society of America Book Series 1. SSSA, Madison, WI.

Brindley, G. W. (1980) Order-disorder in clay mineral structures In G. W. Brindley and Brown G. Eds., Crystal Structures of Clay Minerals and their X-ray Identification, 125 – 195. Mineralogical Society Monography No. 5, Mineralogical Society, London.

Brown, G., Newman, A. C. D., Rayner, J. H., and Weir, A. H. (1978) The structure and chemistry of soil clay minerals In D. J. Greenland and M. H. B. Hayes, Eds., The Chemistry of Soil Constituents, 29 – 178. Wiley, New York.

Cama, J., Ganor, J., Sayora, C., and Lasaga, C. A. (2000) Smectite dissolution kinetics at 80°C and pH 8.8. Geochimica et Cosmochimica Acta, 64, 2701–2717.

Cappelli, C., Yokoyama, S., Cama, J., and Huertas, F. J. (2018) Montmorillonite dissolution kinetics: Experimental and reactive transport modeling interpretation. Geochimica et Cosmochimica Acta 227, 96–122.

Chamley, H. (1989) Clay Sedimentology, Springer-Verlag, Berlin. 623 pp.

Chevrier, V., Poulet, F., and Bibring, J-P. (2007) Early geochemical environment of Mars as determined from thermodynamics of phyllosilicates. Nature, 448, 60-63. doi:10.1038/nature05961

Christidis G. E. and Huff, W. D. (2009) Geological aspects and genesis of bentonites. Elements 5, 93–98.

Devidal, J-C., Dandurand, J-L. and Gout, R. (1996) Gibbs free energy of formation of kaolinite from solubility measurement in basic solution between 60 and 170°C. Geochimica et Cosmochimica Acta, 53, 553-564.

Di Pietroa, S.A., Emerson, H.P., Katsenovich, Y., Qafokub, N.P., and Szecsody J.E. (2020) Phyllosilicate mineral dissolution upon alkaline treatment under aerobic and anaerobic conditions. Applied Clay Science 189, 105520 https://doi.org/10.1016/j.clay.2020.105520

Ehlmann, B. L., and Edwards, C. S. (2014) Mineralogy of the Martian Surface. Annual Reviews in Earth Planetary Sciences, 42, 291–315.

Essene, E. J., and Peacor, D. R. (1995). Clay mineral thermometry: A critical perspective. Clays and Clay Minerals, 43, 540–553.

Foster, M.D. The Relation between Composition and Swelling in Clays. Clays and Clay Minerals **3,** 205–220 (1954). https://doi.org/10.1346/CCMN.1954.0030117

Gaboreau, S., Gailhanou, H., Blanc, Ph., Vieillard, Ph., and Made, B. (2020) Clay mineral solubility from aqueous equilibrium: Assessment of the measured thermodynamic properties. Applied Geochemistry, 113, 104465 https://doi.org/10.1016/j.apgeochem.2019.104465

Gainey, S.R., Hausrath, E.M., Hurowitz, J.A., and Milliken, R.A. (2014) Nontronite dissolution rates and implications for Mars, Geochimica et Cosmochimica Acta 126, 192–211.

Güven, N. (1988) Smectites. Reviews in Mineralogy and Geochemistry, 19, 497 – 559.

Hemingway, B.S., Kittrick, J.A., Grew, E.S., Nelen, J.A., and London, D. (1984) The heat capacity of osumilite from 298.15 to 1000 K, the thermodynamic properties of natural chlorites to 500 K, and the thermodynamic properties of petalite to 1800 K. American Mineralogist, 69, 701–710.

Jeans, C. V. (2009) Contrasting books on clay mineral science – How should they be judged? Acta Geodynamica et Geomaterialia, 6, 45-58.

Kittrick, J. A. (1966) Free energy of formation of kaolinite from solubility measurements. American Mineralogist 51, 1457-1466

Kittrick, J. A. (1969) Soil minerals in the Al_2O_3-SiO_2-H_2O system and a theory of their formation. Clays and Clay Minerals, 17, 157-167

Kittrick, J. A. (1982) Solubility of two high-Mg and two high-Fe chlorites using multiple equilibria: Clays and Clay Minerals 30, 167-179.

Kittrick, J. A. (1984). Solubility measurements of phases in three illites. Clays and Clay Minerals, 32, 115–124.

Kittrick, J.A., and Peryea, F.J. (1988) Experimental validation of the monophase structure model for montmorillonite solubility. Soil Science Society of America Journal, 52, 1199-1201.

Kittrick, J. A. and Peryea, F. J. (1989) The monophase structure model for Mg^{2+}-saturated montmorillonite. Soil Science Society of America Journal, 53, 292 - 295.

Köhler, S. J., Bosbach, D., and Oelkersm E. H. (2005) Do clay mineral dissolution rates reach steady state? Geochimica et Cosmochimica Acta, 69, 1997–2006.

Köhler, S. J., Bosbach, D., and Oelkers, E. H. (2005) Do clay mineral dissolution rates reach steady state? Geochimica et Cosmochimica Acta, 69, 1997–2006.

Lippmann, F. (1977) The solubility products of complex minerals, mixed crystals, and three-layer clay minerals. Neues Jahrbuch für Mineralogie – Abhandlungen, 130, 243-263.

Lippmann, F. (1982) The thermodynamic status of clay minerals: Proc. 7th Int. Clay Conf., 1981, pp. 475-485.

May, H. M. (1978) Aluminum determination, aluminum hydrolysis and the solubilities of some common aluminous minerals in near-neutral aqueous solutions. Ph.D. Dissertation, The University of Wisconsin, Madison, WI.

May H.M. and Nordstrom D.K. (1991) Assessing the solubilities and reaction kinetics of aluminous minerals in soils. In Ulrich B., Sumner M.E., Eds. Soil Acidity. Springer, Berlin, Heidelberg. https://doi.org/10.1007/978-3-642-74442-6_6

May, H.H., Kinniburgh, D.G., Helmke, P.A., and Jackson, M.L. (1986) Aqueous dissolution, solubilities and thermodynamic stabilities of common aluminosilicate clay minerals: Kaolinite and smectites. Geochimica et Cosmochimica Acta, 50, 1667-1677.

McBride, M.B., and Baveye, P. (2002) Diffuse double-layer model, long range forces, and ordering in clay colloids. Soil Science Society of America Journal 66, 1207-1217.

Metz, V., Amram, K., and Ganor, J. (2005) Stoichiometry of smectite dissolution reaction. Geochimica et Cosmochimica Acta, 69, 1755–1772.

Morse, J. W. and Casey, W. H. (1988). Ostwald processes and mineral paragenesis in sediments. American Journal of Science, 288, 537–560.

Mosser-Ruck, R., Pignatelli, I. Bourdelle, F., Abdelmoula, M., Barres, O., Guillaume, D., Charpentier, D., Rousset, D., Cathelineau, M., and Michau, N. (2016) Contribution of long-term hydrothermal experiments for understanding the smectite - to - chlorite conversion in geological environments. Contributions to Mineralogy and Petrology 171:97 DOI 10.1007/s00410-016-1307-z.

Nordstrom, D.K., and Munoz, J. L. (1994) Geochemical Thermodynamics. 493 pp. Blackwell Scientific Publications. Oxford.

Norrish, K. (1954) The swelling of montmorillonite. Faraday Discussions of Chemical Society, 8, 120-134.

Peryea, F.J. and Kittrick, J.A. (1986) Experimental evaluation of two operational standard states for montmorillonite in metastable hydrolysis reactions. Soil Science Society of America Journal, 50, 1613-1617.

Ransom, B., and Helgeson, H. C. (1993) Compositional endmembers and thermodynamic components of illite and dioctahedral aluminous smectite solid solutions Clays and Clap Minerals, 41, 5, 537-550.

Sass, B. M., Rosenberg, P. E., and Kittrick, J.A. (1987) The stability of illite/smectite during diagenesis: An experimental study: Geochimica et Cosmochimica Acta 51, 2103-2115.

Savage, D., Wilson, J., Benbow, S., Sasamoto, H., Oda, C., Walker, C., Kawama, D., and Tachi, Y. (2019) Natural systems evidence for the effects of temperature and the activity of aqueous silica upon montmorillonite stability in clay barriers for the disposal of radioactive wastes. Applied Clay Science, 179, 105146.

Slade, P.G., and Quirk, J. P. (1991) The limited crystalline swelling of smectites in $CaCl_2$, $MgCl_2$, and $LaCl_3$ solutions Journal of Colloid and Interface Science, 144, 18-26

Smalley, M. V. (1994) Electrical theory of clay swelling. Langmuir, 10, 2884-2891.

Thorstensen, D.C. and Plummer, L.N. (1977) Equilibrium criteria for two-component solids reacting with fixed composition in an aqueous phase-example: The magnesian calcites: American Journal pf Science, 277, 1203-1223.

Wilson, M. J. (2013) Rock Forming Minerals, Vol. 3c, Sheet Silicates–Clay Minerals, 2nd edition. The Geological Society London, 724 pp.

Wilson, J., Savage, D., Cuadros, J., Shibata, M., and Ragnarsdottir, K.V. (2006a) The effect of iron on montmorillonite stability: I. Background and thermodynamic considerations. Geochimica et Cosmochimica Acta, 70, 306–322

Wilson, J., Cressey, G., Cressey, B., Cuadros, J., Ragnarsdottir, K. V., Savage, D., and Shibata, M. (2006b) The effect of iron on montmorillonite stability. II. Experimental investigation. Geochimica et Cosmochimica Acta, 70, 323–336.

Yates, D.M., and Rosenberg, P.E. (1998). Characterization of neoformed illite from hydrothermal experiments at 250 °C and $P_{v=soln}$: An HRTEM/ATEM study. American Mineralogist, 83, 1199–1208

LIST OF FIGURES

Figure 1. Isothermal, isobaric, ion activity diagrams depicting compositions of aqueous solutions equilibrated with chlorite-kaolinite mineral mixtures (Aja and Dyar, 2002): a) Windsor – kaolinite equilibria at 75 °C, b) clinochlore (low-Fe) – kaolinite equilibria at 25

This is the peer-reviewed, final accepted version for American Mineralogist, published by the Mineralogical Society of America.
The published version is subject to change. Cite as Authors (Year) Title. American Mineralogist, in press.
DOI: https://doi.org/10.2138/am-2022-8213. http://www.minsocam.org/

°C. In both cases, the experimental data validate predicted slopes for chlorite-kaolinite equilibria.

Figure 2. Depiction of solubility data of Mg-saturated BF montmorillonite $[Mg_{0.47}(Si_{7.55}Al_{0.45})(Al_{3.15}Mg_{0.61}Fe_{0.28})O_{20}(OH)_4]$ equilibrated with gibbsite and goethite, at 25 °C (Kittrick and Peryea, 1989), in 2pH-pMg^{2+} vs. pH_4SiO_4 space.

Figure 3. Graphical evaluation of smectite MX-80 dissolution data at 25 °C reported by Gaboreau et al. (2020): a) 3pH-pAl^{3+} vs. pH_4SiO_4 space, b) 2pH-pMg^{2+} vs. pH_4SiO_4 space. In the former ion activity space, the fitted and model slopes are 1.88(0.50) and 2.01, respectively whereas in the latter, the model and fitted slopes are 17.47 and 1.50(0.57), respectively. At the 95% confidence level, the data projected onto the 3pH-pAl^{3+} vs. pH_4SiO_4 space are in agreement with the predicted value whereas there is no agreement between the slope of the best-fit and predicted slope in 2pH-pMg^{2+} vs. pH_4SiO_4.

Figure 4. Graphical evaluation of solubility data of Santa Ollala vermiculite and CCa-2 chlorite at 25 °C (Gaboreau et al. 2020): a) 2pH-pMg^{2+} vs pH_4SiO_4 plot for Santa Ollala vermiculite, b) 2pH – pMg^{2+} vs. pH_4SiO_4 plot of CCa-2 chlorite, and c) combined plots for SO and CCa-2 solubility data on 2pH – pMg^{2+} vs. pH_4SiO_4 coordinates. The slope of best fit line to SO solubility data has a slope of 9.63(0.82) at the 95% confidence level which is rather different from the model value of 1.11. For CCa-2, the best fit line has a negative slope of -3.37(0.84), at the 95% confidence level, which is diametrically opposed to the predicted positive slope of 0.89. The overlap of their solubility data for the vermiculite and chlorite (c) suggests likelihood of similarities in the identity of the solubility-controlling phases.

Figure 5. $\log \frac{a_{Mg^{2+}}^{0.5}}{a_{H^+}}$ vs. $\log a_{SiO_{2(aq)}}$ diagrams showing directions from which the equilibrium solution compositions were approached. Open circles show final solution compositions whereas solid circles indicate starting fluid compositions in which aqueous silica was present. Arrows indicate directions of approach for runs in which silica was not present.

Figure 6. Changes in pH of solutions reacted with chlorite-kaolinite mixtures at 125 °C. The arrows show the overall directions rather than trajectories of pH changes resulting from fluid-mineral equilibration. Open circles and squares represent equilibrium pH values re-cal-culated from quench pH whereas filled circles and squares indicate the pH of starting solutions. Experiments conducted in NaCl and $MgCl_2$ solutions are shown as circles and squares, respectively. Sources of experimental data: Aja and Small (1999) and Aja and Dyar (2002).

Figure 7. 3pH – pAl^{3+} vs. pH_4SiO_4 plot of KGa-2 solubility data (Gaboreau et al., 2020). For stoichiometric kaolinite, the appropriate solubility model is: $Al_2Si_2O_5(OH)_4 + 6H^+ \rightleftharpoons$

1017 $2Al^{3+} + 2H_4SiO_4 + H_2O$ which yields a solubility product expression of the form, 3pH –
1018 $pAl^{3+} = pH_4SiO_4 + 0.5pK$. The solubility model predicts a positive slope of 1 rather than
1019 the slope of 2.22(0.63), at the 95% confidence level, returned by the best-fit analysis.
1020 The dot-dashed line shows a line drawn through the solubility data having the
1021 appropriate slope of unity. The stoichiometry of the kaolinite used in the investigation
1022 was reported $Al_{1.98}Si_2Fe_{0.02}O_{4.99}(OH)_4$ which changes the predicted slope to 1.01
1023 instead of 1.
1024

This is the peer-reviewed, final accepted version for American Mineralogist, published by the Mineralogical Society of America.
The published version is subject to change. Cite as Authors (Year) Title. American Mineralogist, in press.
DOI: https://doi.org/10.2138/am-2022-8213. http://www.minsocam.org/

1025 # Table 1: Solubility equilibrium models of some multicomponent layer silicates

Mineral sample	Solubility models and corresponding equilibrium constant expressions	Eqn. No
Windsor chamosite	$(Fe^{3+}_{0.60}Fe^{2+}_{5.43}Mg_{2.30}Al_{2.98}Mn_{0.05}Ca_{0.03}Zn_{0.01}\square_{0.60})(Si_{5.63}Al_{2.37})O_{20}(OH)_{16} + 1.42\ O_{2\,(g)} + 4.59\ H_2O + 1.27\ H^+_{(aq)} \rightleftharpoons Al_2Si_2O_5(OH)_4 + 3.35\ Al(OH)^-_4 + 3.63\ SiO_{2\,(aq)} + 2.30\ Mg^{2+} + 4.52\ FeOOH + 1.51\ Fe(OH)^\circ_{3\,(aq)} + 0.05\ MnO^-_4 + 0.01\ Zn^{2+} + 0.03\ Ca^{2+}$	**1**
	$\log\frac{a^{0.5}_{Mg^{2+}}}{a_{H^+}} = -1.46\log(a_{Al(OH)^-_4})(a_{H^+}) - 1.58\log a_{SiO_{2(aq)}} - 0.66\log a_{Fe(OH)^\circ_{3\,(aq)}} - 0.02\log(a_{MnO^-_4}\cdot a_{H^+}) - 0.004\log\frac{a^{0.5}_{Zn^{2+}}}{a_{H^+}} - 0.01\log\frac{a^{0.5}_{Ca^{2+}}}{a_{H^+}} + 0.62\log f_{O_2} + 0.43\ \log K_1$	**2**
Belle Fourche montmorillonite	$Mg_{0.47}(Si_{7.55}Al_{0.45})(Al_{3.15}Mg_{0.61}Fe_{0.28})O_{20}(OH)_4 + 2.16\ H^+_{(aq)} + 17.56\ H_2O = 3.60\ Al(OH)_{3\,(s)} + 0.28\ FeOOH_{(s)} + 1.08\ Mg^{2+}_{(aq)} + 7.55\ Si(OH)^\circ_4$	3
	$2pH - pMg^{2+} = 6.99\ pSi(OH)^\circ_4 - 0.93\ pK_3$	4
MX-80 smectite	$Na_{0.409}K_{0.024}Ca_{0.009}(Si_{3.738}Al_{0.262})(Al_{1.598}Mg_{0.214}Fe_{0.208})O_{10}(OH)_2 \bullet 5.189H_2O + 7.04H^+_{(aq)} \rightarrow 1.86Al^{3+}_{(aq)} + 3.738H_4SiO_{4(aq)} + 0.035Fe^{2+}_{(aq)} + 0.173Fe^{3+}_{(aq)} + 0.214Mg^{2+}_{(aq)} + 0.409Na^+_{(aq)} + 0.024K^+_{(aq)} + 0.009Ca^{2+}_{(aq)} + 2.237H_2O$	5
	$3pH - pAl^{3+} = 2.01pH_4SiO_4 - 0.019\ (2pH - pFe^{2+}) - 0.093\ (3pH - pFe^{3+}) - 0.115\ (2pH - pMg^{2+}) - 0.220\ (pH - pNa^+) - 0.013\ (pH - pK^+) - 0.005(2pH - pCa^{2+}) - 0.538pK_5$	6

This is the peer-reviewed, final accepted version for American Mineralogist, published by the Mineralogical Society of America.
The published version is subject to change. Cite as Authors (Year) Title. American Mineralogist, in press.
DOI: https://doi.org/10.2138/am-2022-8213. http://www.minsocam.org/

Vermiculite SO	$Ca_{0.445}(Si_{2.778}Al_{1.222})(Al_{0.216}Mg_{2.475}Fe_{0.254})O_{10}(OH)_2 + 10.888H^+_{(aq)} \rightarrow 1.438\ Al^{3+}_{(aq)} + 2.778\ H_4SiO_{4\,(aq)} + 0.028Fe^{2+}_{(aq)} + 0.226\ Fe^{3+}_{(aq)} + 2.475Mg^{2+}_{(aq)} + 0.445\ Ca^{2+}_{(aq)} + 0.888\ H_2O_{(l)}$	8
	$2pH - pMg^{2+} = 1.12\ pH_4SiO_4 - 0.58\ (3\ pH - pAl^{3+}) - 0.01\ (2pH - pFe^{2+}) - 0.09\ (3pH - pFe^{3+}) - 0.18\ (2pH - pCa^{2+}) - 0.40\ pK_8$	9
Chlorite CCa-2	$(Mg_{2.964}Fe_{1.927}Al_{1.116}Ca_{0.011})(Si_{2.633}Al_{1.367})O_{10}(OH)_8 + 17.468H^+ \rightarrow 2.483Al^{3+} + 2.633H_4SiO_4 + 1.712Fe^{2+} + 0.215Fe^{3+} + 2.964Mg^{2+} + 0.011Ca^{2+} + 7.468H_2O$	10
	$2pH - pMg2+ = 0.89\ pH_4SiO_4 - 0.84\ (3pH - pAl^{3+}) - 0.58\ (2pH - pFe^{2+}) - 0.07\ (3pH - pFe^{3+}) - 0.004\ (2pH - pCa^{2+}) - 0.34\ pK_{10}$	11

1026

1027

1028 Table 2: Fluid – solid ratios in some recent solubility studies of complex layer silicates

Cited Studies	**Minerals investigated**	**Type of solubility experiments**	**Fluid to solid ratio**	**Duration of experiments**	**Comments**
May et al. (1986)	1. Upton (WY) bentonite 2. Panther Creek (MI) bentonite 3. Kokokahi (HI) soil 4. Lualualei (HI) soil 5. St. Louis Heights (HI) soil	Direct dissolution; final solution composition approached from over and undersaturation.	100:1	2 – 419 days at 25 °C	Irrational solubility pattern reported for all five smectite samples.
Kittrick and Peryea (1989)	Belle-Fourche montmorillonite (BF)	Solution equilibration techniques (BF + goethite + gibbsite); final solution composition approached from over and undersaturation.	1:1.3	7 – 15 days at 25 °C	Solubility data consistent with monophase model of smectite solubility.
Gaboreau et al. (2020)	MX-80 smectite	Sample dissolution in acidified NaCl solution (pH ≅5); final solution composition approached from undersaturation.	24:1	1 – 2500 days at 25 °C	Rational solubility behavior: the predicted slopes of chemical potential diagram consistent with solubility data.
	Santa Ollala vermiculite	Sample dissolution in acidified $CaCl_2$ (pH ≅5). Final solution composition approached from one direction.	24:1	1 – 2500 days at 25 °C	Rational solubility data but the predicted slope of chemical potential diagram differs significantly from measured value.
Aja and Small (1999); Aja and Dyar (2002)	1. Low-Fe clinochlore 2. High-Mg chamosite	Solution equilibration of the chlorites with kaolinite (±quartz ± gibbsite ± hematite); final solution composition approached from over and undersaturation.	Varied between 2.4:1 and 1.8:1	90 – 430 days spanning 25 to 200 °C.	Predicted slopes of kaolinite - chlorite boundaries in agreements with solution equilibration data at all temperatures studied.

This is the peer-reviewed, final accepted version for American Mineralogist, published by the Mineralogical Society of America.
The published version is subject to change. Cite as Authors (Year) Title. American Mineralogist, in press.
DOI: https://doi.org/10.2138/am-2022-8213. http://www.minsocam.org/

Figure 1a

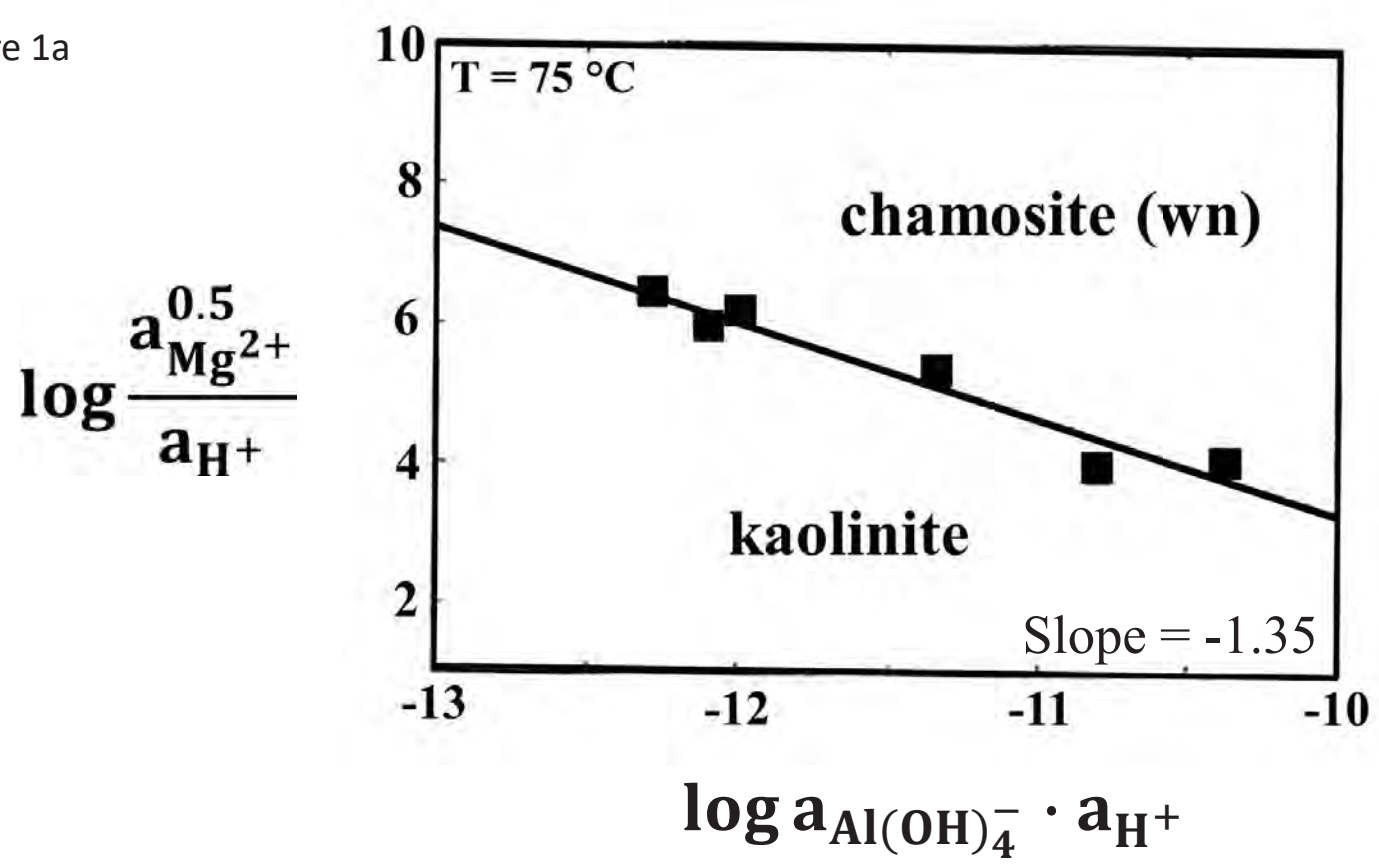

This is the peer-reviewed, final accepted version for American Mineralogist, published by the Mineralogical Society of America.
The published version is subject to change. Cite as Authors (Year) Title. American Mineralogist, in press.
DOI: https://doi.org/10.2138/am-2022-8213. http://www.minsocam.org/

Figure 1b

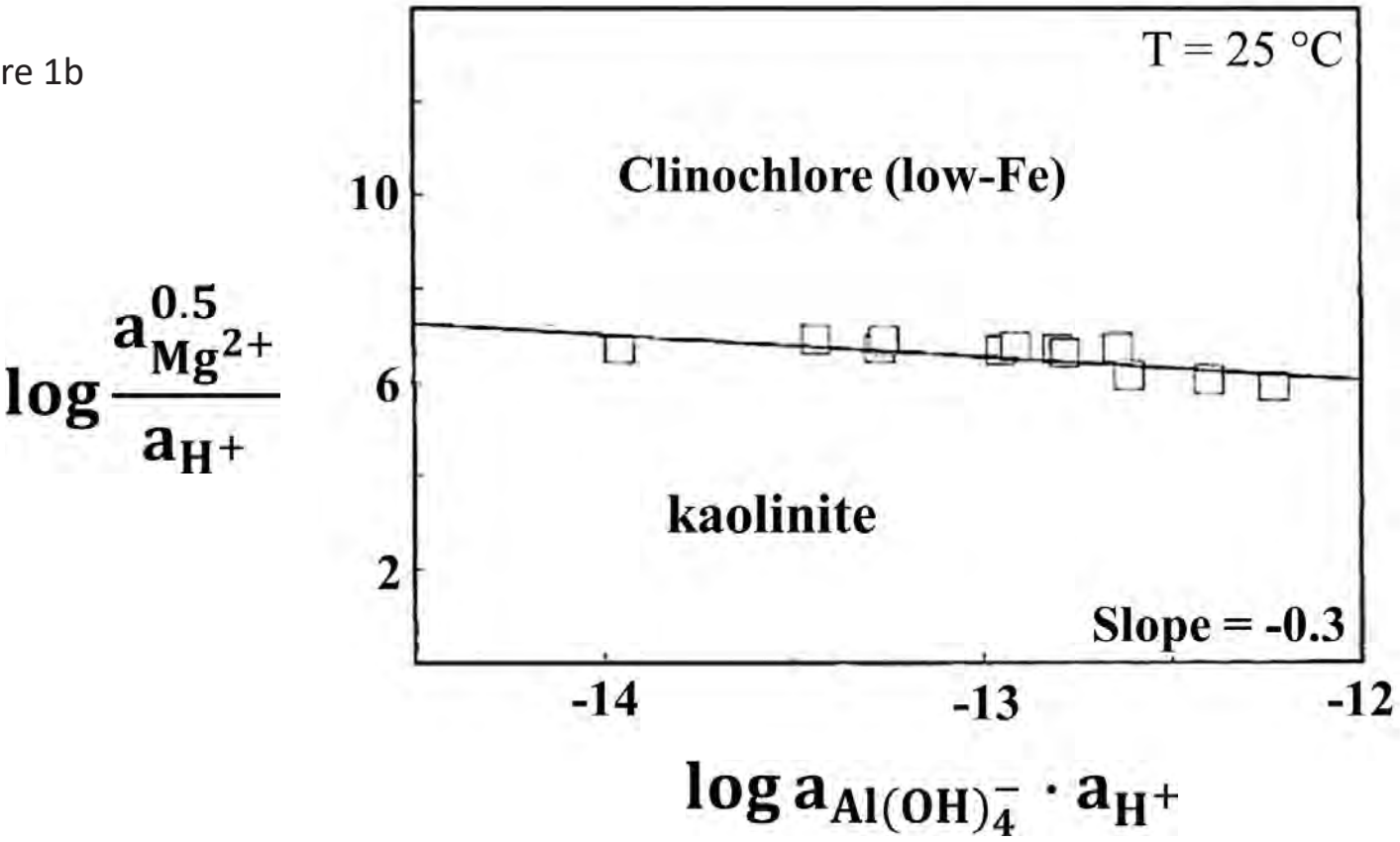

This is the peer-reviewed, final accepted version for American Mineralogist, published by the Mineralogical Society of America.
The published version is subject to change. Cite as Authors (Year) Title. American Mineralogist, in press.
DOI: https://doi.org/10.2138/am-2022-8213. http://www.minsocam.org/

Figure 2

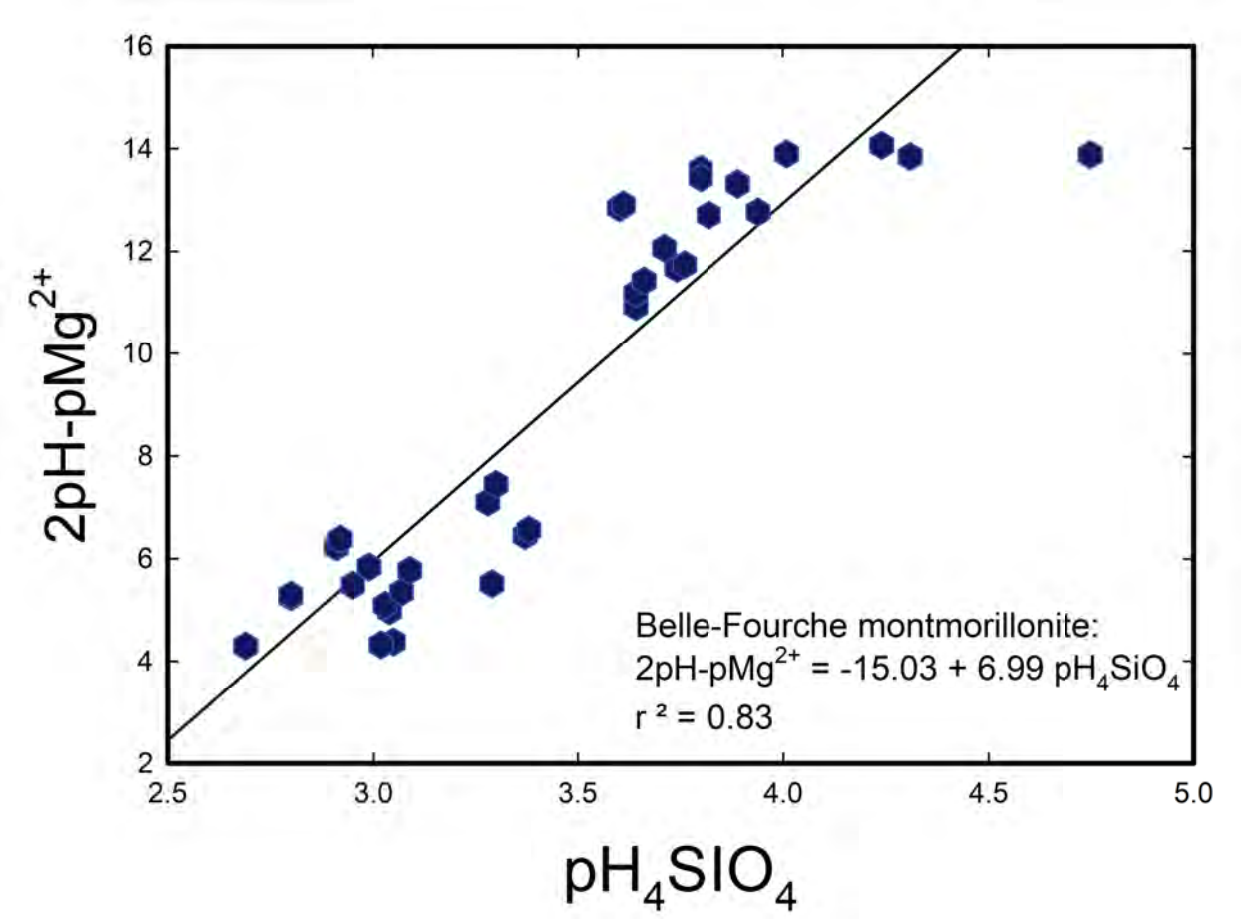

This is the peer-reviewed, final accepted version for American Mineralogist, published by the Mineralogical Society of America.
The published version is subject to change. Cite as Authors (Year) Title. American Mineralogist, in press.
DOI: https://doi.org/10.2138/am-2022-8213. http://www.minsocam.org/

Figure 3a

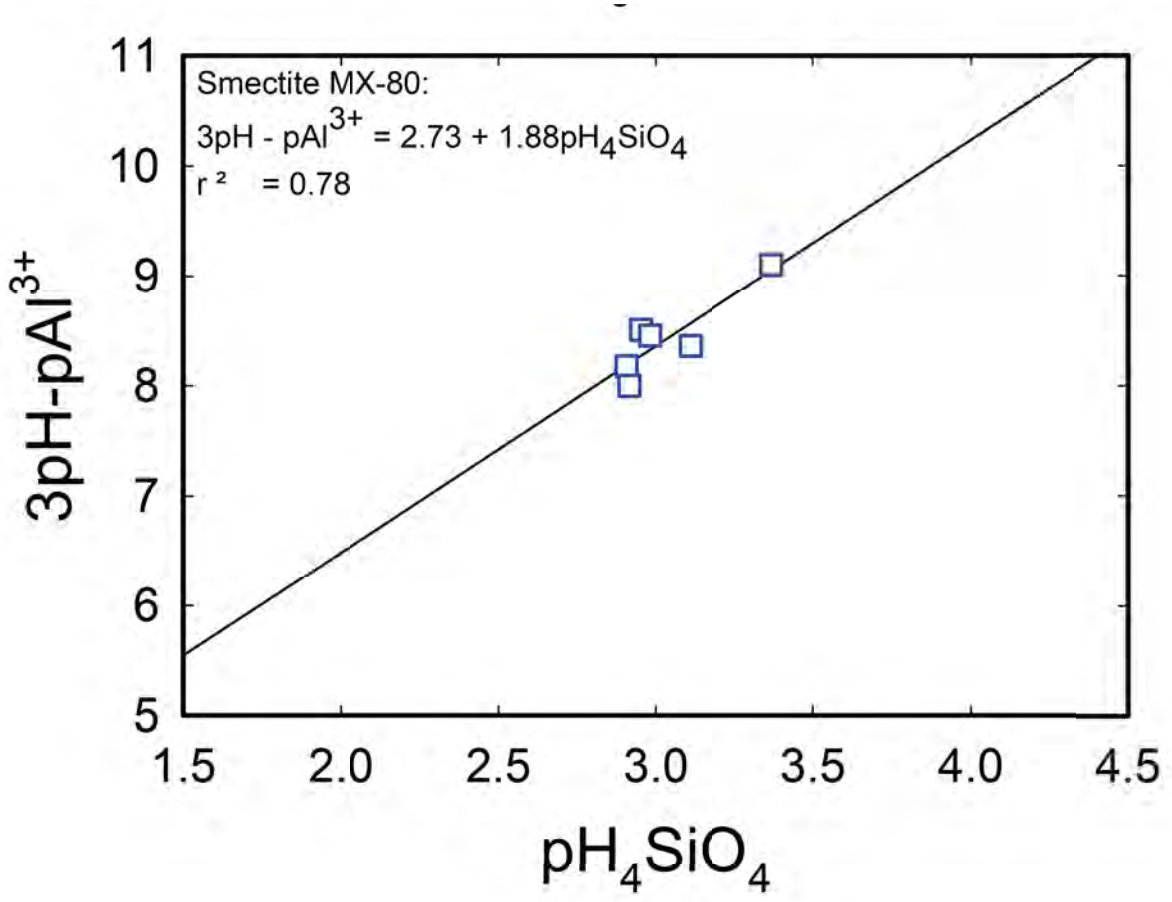

This is the peer-reviewed, final accepted version for American Mineralogist, published by the Mineralogical Society of America.
The published version is subject to change. Cite as Authors (Year) Title. American Mineralogist, in press.
DOI: https://doi.org/10.2138/am-2022-8213. http://www.minsocam.org/

Figure 3b

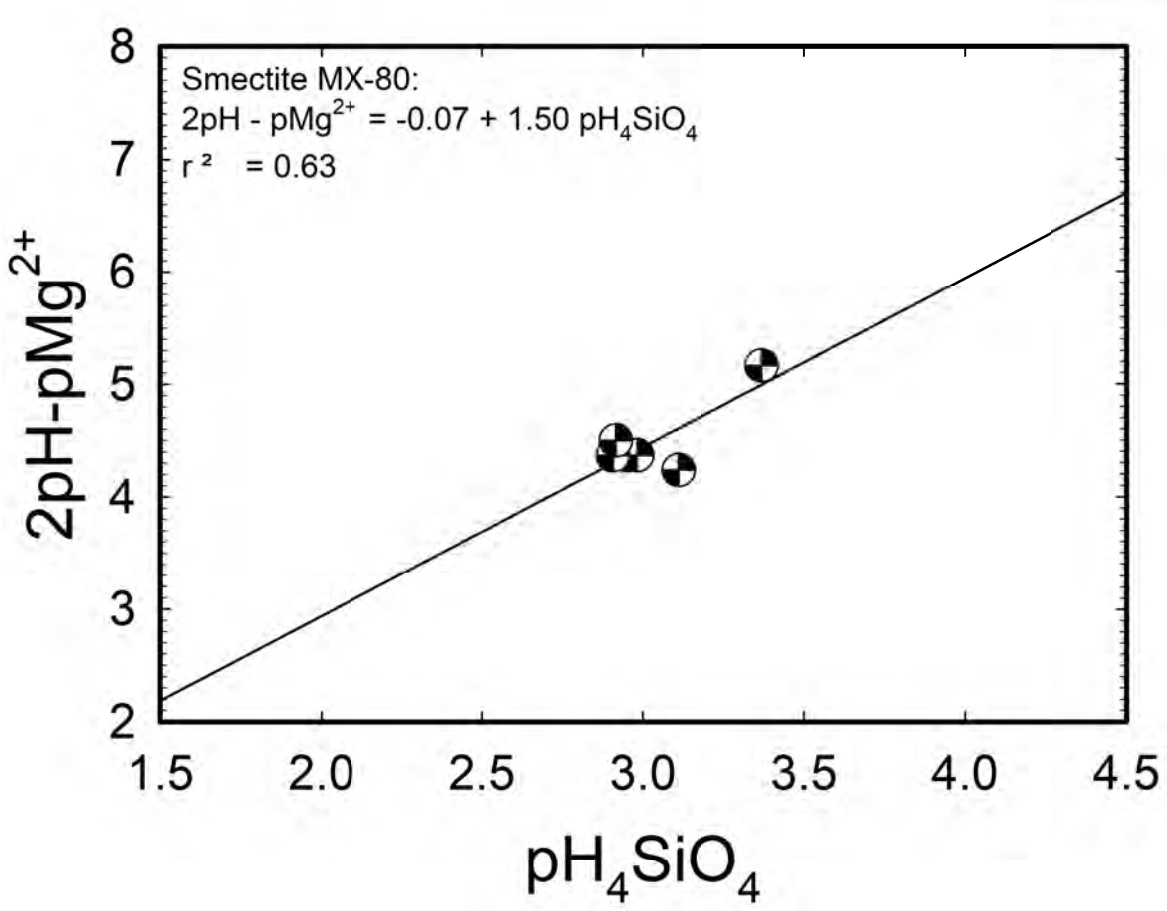

This is the peer-reviewed, final accepted version for American Mineralogist, published by the Mineralogical Society of America.
The published version is subject to change. Cite as Authors (Year) Title. American Mineralogist, in press.
DOI: https://doi.org/10.2138/am-2022-8213. http://www.minsocam.org/

Figure 4a

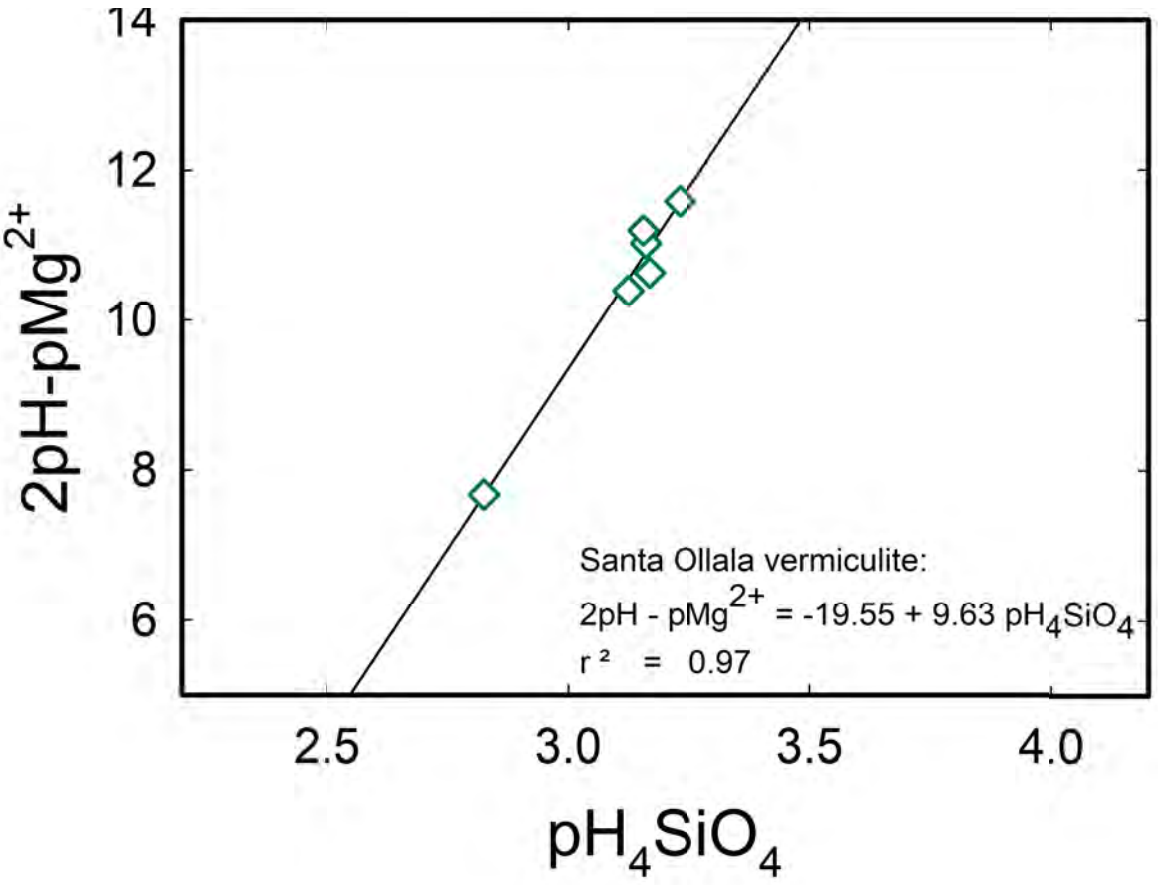

This is the peer-reviewed, final accepted version for American Mineralogist, published by the Mineralogical Society of America.
The published version is subject to change. Cite as Authors (Year) Title. American Mineralogist, in press.
DOI: https://doi.org/10.2138/am-2022-8213. http://www.minsocam.org/

Figure 4b

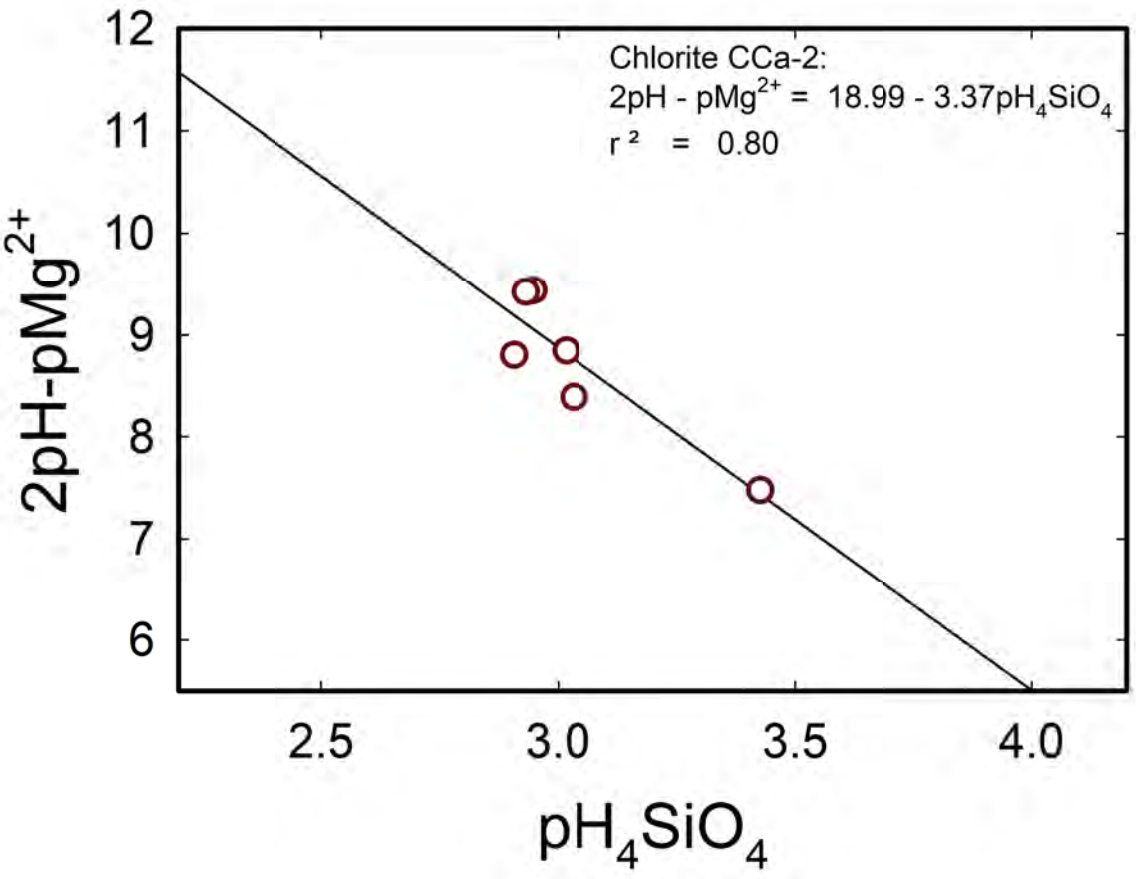

This is the peer-reviewed, final accepted version for American Mineralogist, published by the Mineralogical Society of America.
The published version is subject to change. Cite as Authors (Year) Title. American Mineralogist, in press.
DOI: https://doi.org/10.2138/am-2022-8213. http://www.minsocam.org/

Figure 4c

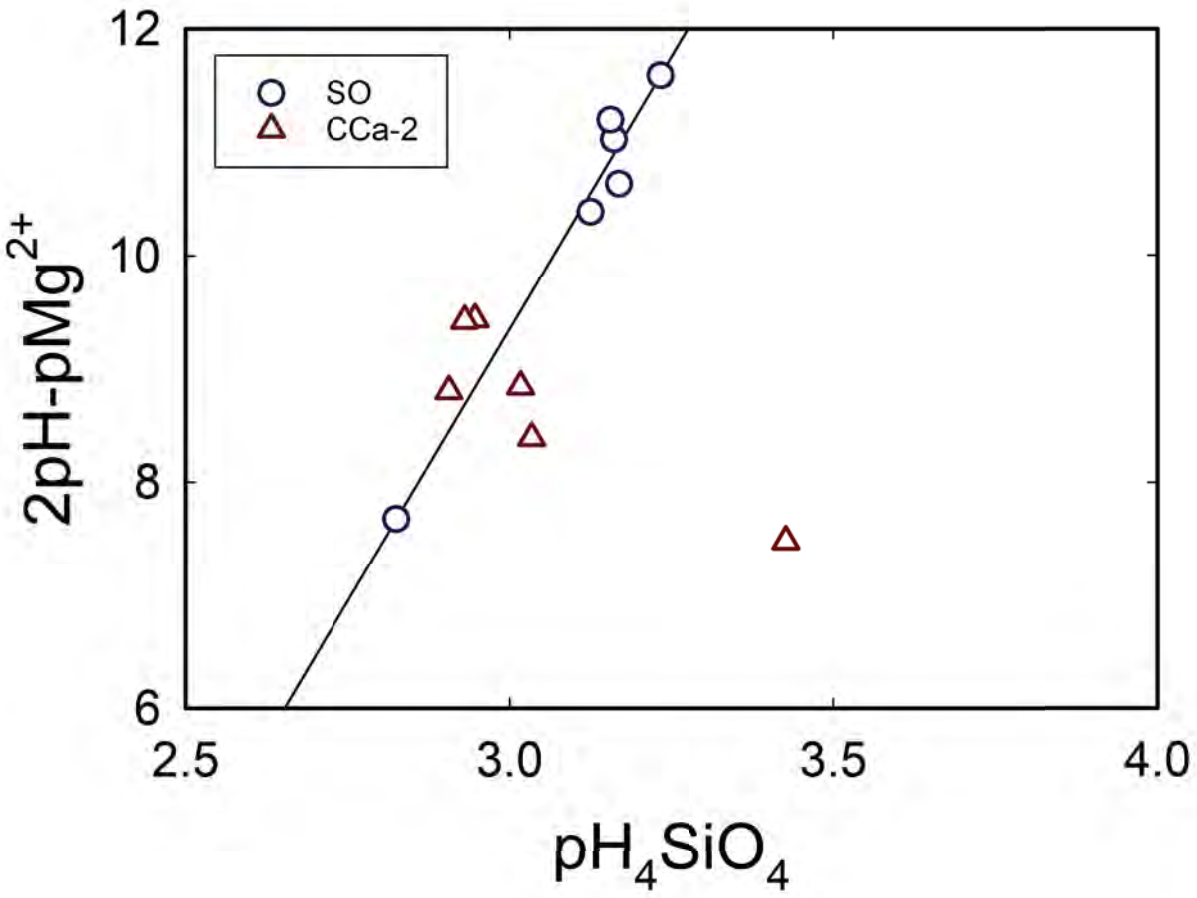

This is the peer-reviewed, final accepted version for American Mineralogist, published by the Mineralogical Society of America.
The published version is subject to change. Cite as Authors (Year) Title. American Mineralogist, in press.
DOI: https://doi.org/10.2138/am-2022-8213. http://www.minsocam.org/

Figure 5

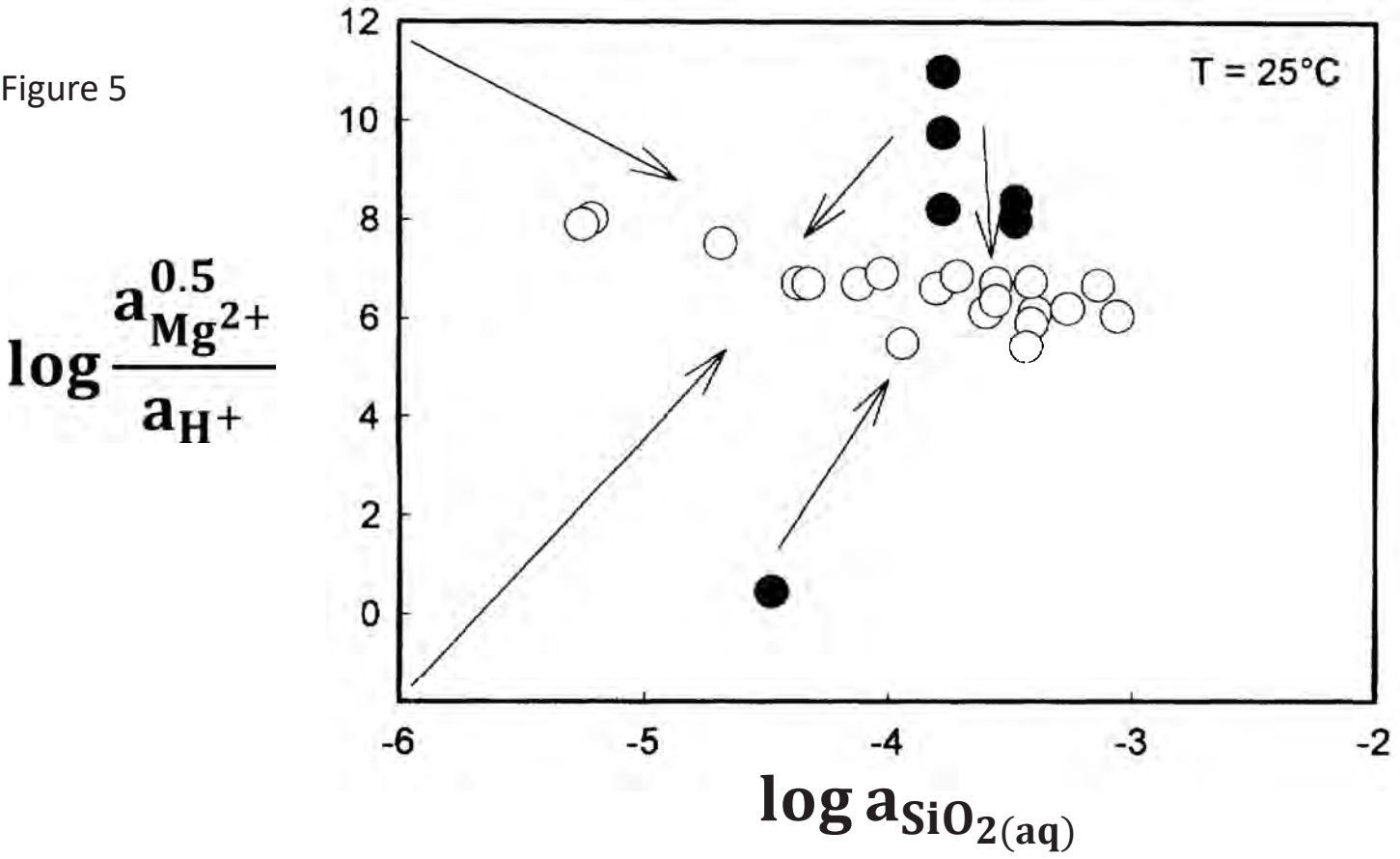

This is the peer-reviewed, final accepted version for American Mineralogist, published by the Mineralogical Society of America.
The published version is subject to change. Cite as Authors (Year) Title. American Mineralogist, in press.
DOI: https://doi.org/10.2138/am-2022-8213. http://www.minsocam.org/

Figure 6

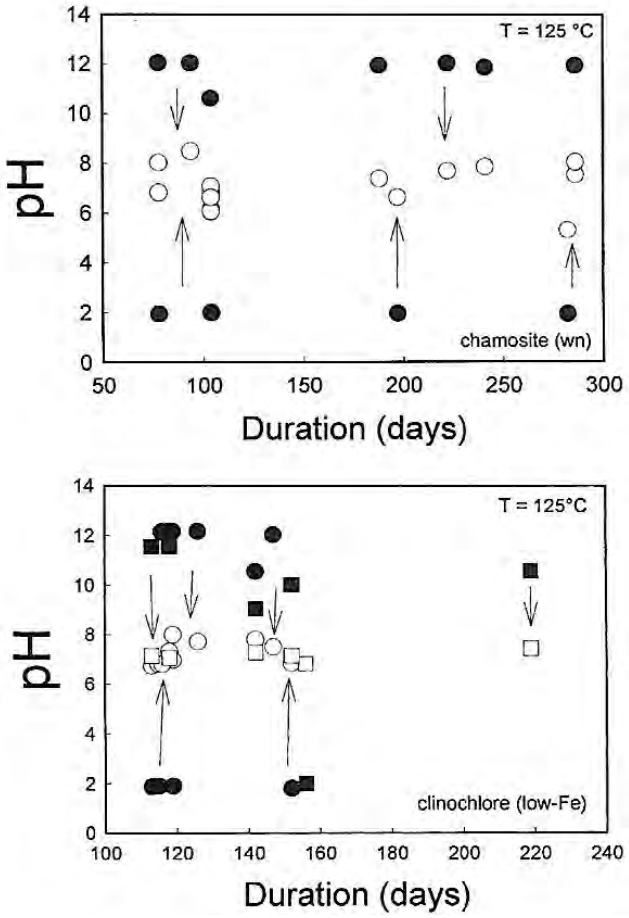

This is the peer-reviewed, final accepted version for American Mineralogist, published by the Mineralogical Society of America.
The published version is subject to change. Cite as Authors (Year) Title. American Mineralogist, in press.
DOI: https://doi.org/10.2138/am-2022-8213. http://www.minsocam.org/

Figure 7